April 19, 2022 Online Low Temperature Plasma Seminar

Magnetic nozzle (MN) helicon plasma thruster

Kazunori Takahashi
Department of Electrical Engineering, Tohoku University
Email: Kazunori.Takahashi.e8@tohoku.ac.jp

Kazu's hand-made plasma reactors

Working with 4 master course students.

Electric propulsion
Plasma physics (propulsion, space, etc…)
Industrial plasmas

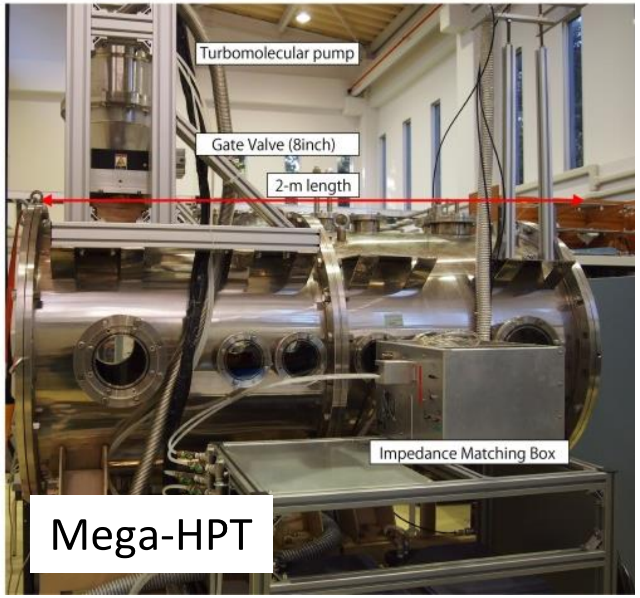

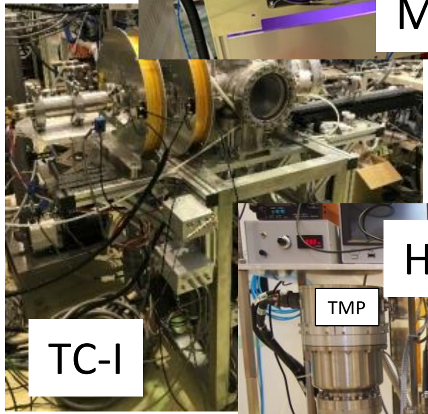

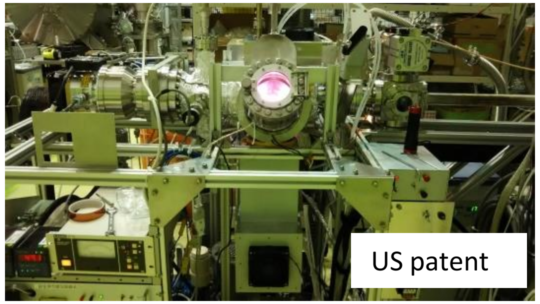

Ultra High vacuum sputtering

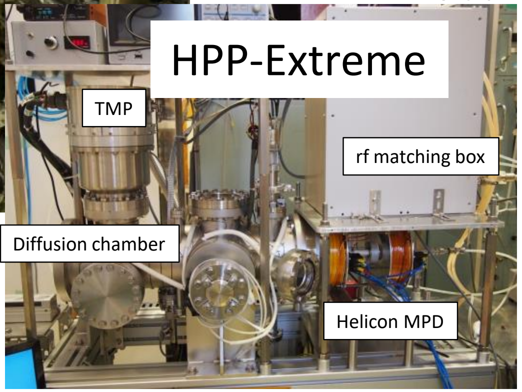

RF system
Development

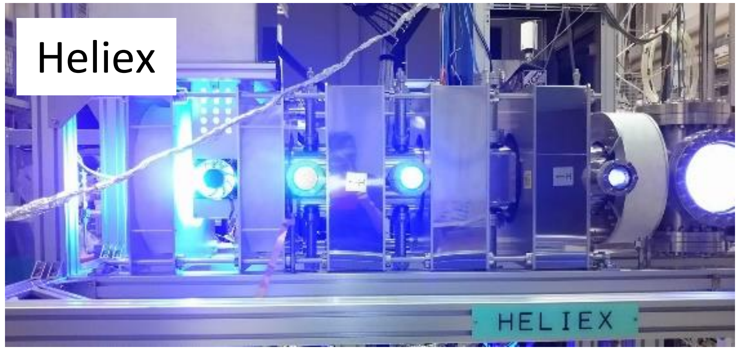

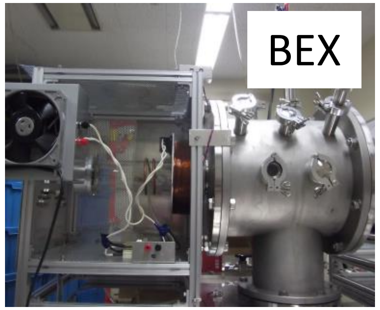

Helicon plasma thruster

Fundamental physics

Plasma-neutral interaction (APL2016x2)

Pressure force (APL2011)

Diamagnetic thrust (PRL2011, POP2012, PRL2013)

Stretching the magnetic field (PRL2017)

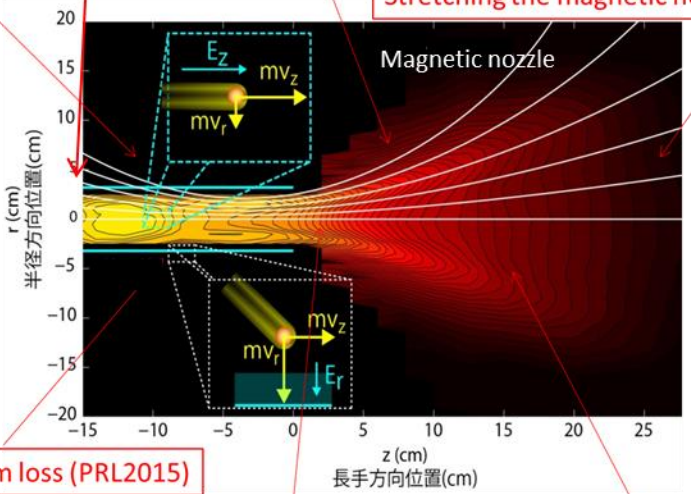

Momentum loss (PRL2015)

Spontaneous charge neutralization (PoP2007, PRL2011)

Electron thermodynamics (PRL2018, PRL2020)

New application

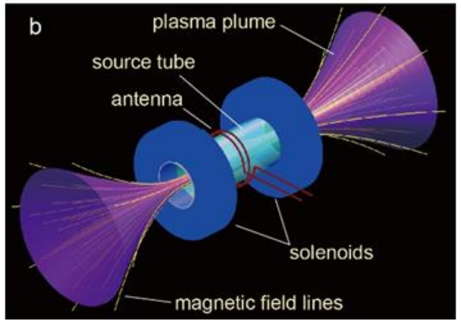

Space debris removal
(Sci. Rep. 2018)

Engineering

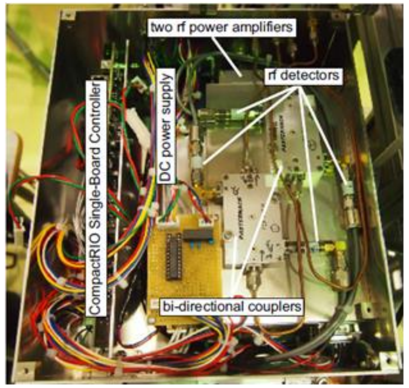

Automatically-controlled RF system
(Front.Phys. 2021)

Magnetic nozzle thruster includes many aspects of physics and engineering

- ✓ Thrust generation mechanisms
- ✓ Performance improvement
- ✓ Electron thermodynamics in the magnetic nozzle
- ✓ Plasma detachment from the magnetic nozzle
- ✓ Application to space debris removal
- ✓ RF engineering

Thrust

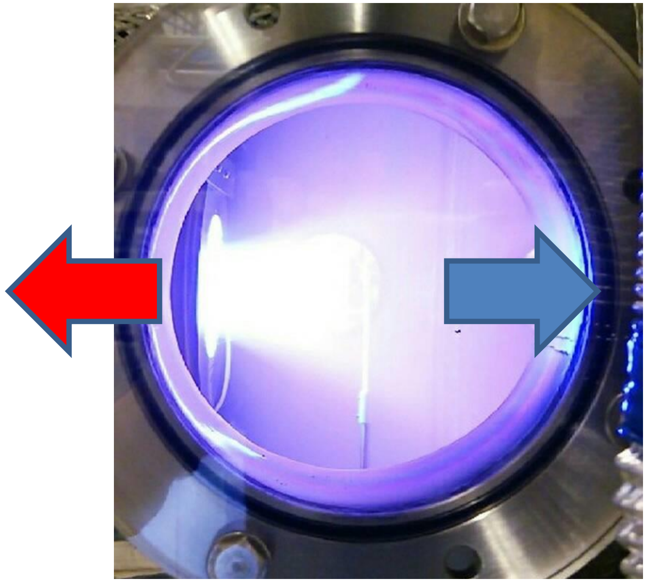

- Thrust F is equal in magnitude and opposite in direction to the momentum flux exhausted from the system.
- Momentum flux M of the fluid is given by sum of the static pressure (nk_BT) and dynamic pressure (mnv^2)

$$F = M = (nk_BT + mnv^2)*A$$

- For helicon thruster ($T_e >> T_i$), the ion pressure and the electron dynamic pressure would be negligible;

$$F = M = (\underbrace{nk_BT_e}_{\text{electron pressure}} + \underbrace{m_inu_z^2}_{\text{ion dynamic pressure}})*A$$

The thrust is the reaction force of the ejected momentum per unit time.
This force is exerted to somewhere in the thruster and somehow.

Energy/Momentum flow in the system

DC power

RF Engineer

RF power

Circuit loss (10%)

Ion heating (negligible)

Electron heating (90%)

Plasma Production

Parallel pressure/energy

Electrostatic Ion acceleration

Ion dynamic momentum via an electrostatic field

Loss to the radial wall (negative thrust)

Perpendicular pressure/energy

Ion dynamic momentum via a sheath (near the wall)
(does not affect the thrust directly)

Radially directed momentum in the MN
(does not affect the thrust directly)

Momentum conversion via a magnetic expansion

Magnetic nozzle

Ionization, Excitation

Atomic Processes

1-D dynamics of electrons and ions

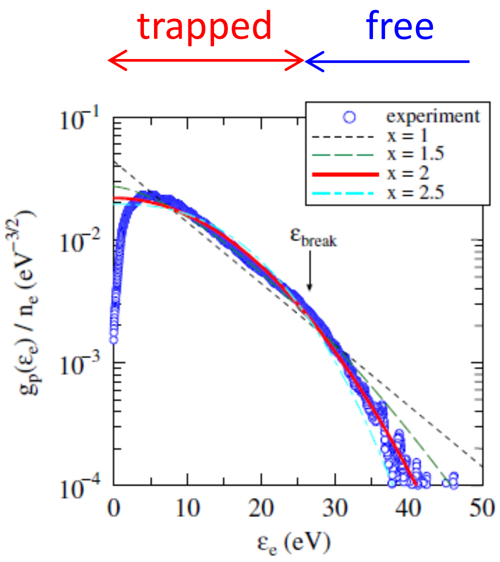

Takahashi et al., POP2007
Takahashi et al., PRL2011a
Boswell et al., FPP 2015

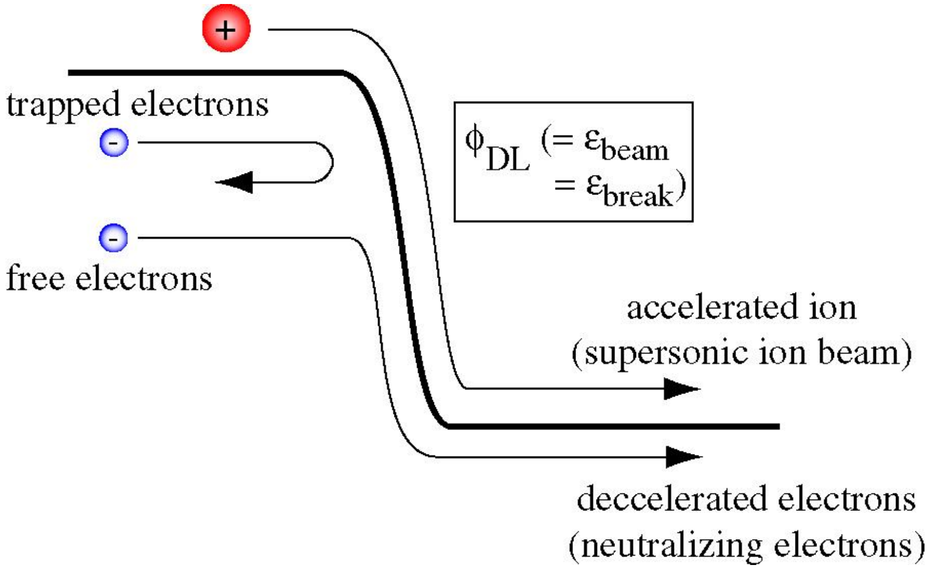

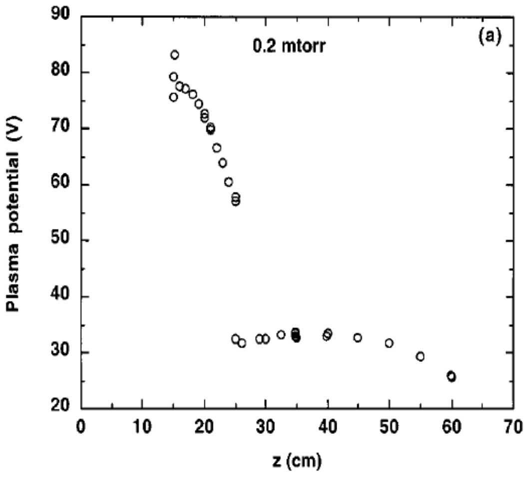

Charles and Boswell, APL2003

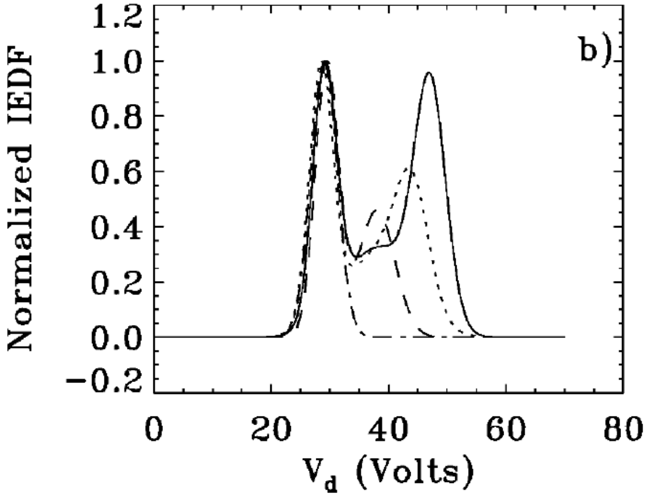

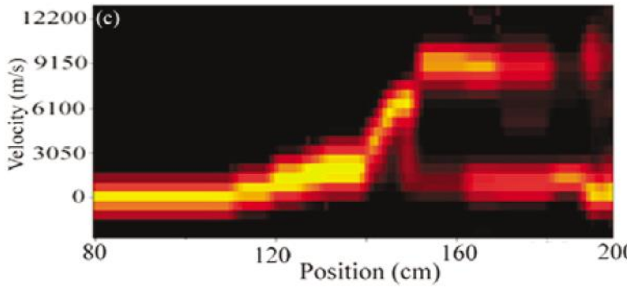

Charles and Boswell, POP2004
Sun et al., PRL2005

2-D Nature of the plume in the MN

Ions

Cox et al., APL2008

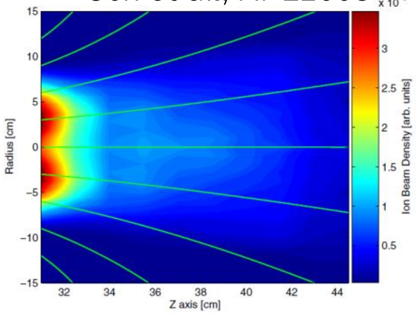

Charles et al, PRL2009

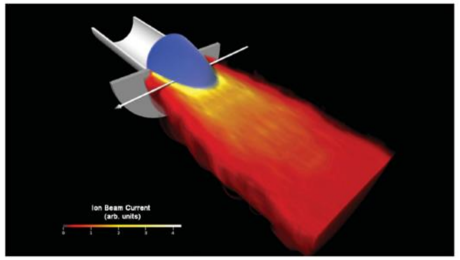

Takahashi et al., JPD2011

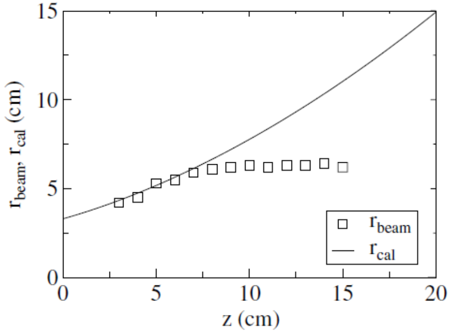

Collimated ion beam is detected.
The ions seem to be deviated from the MN.

Electrons

APL2009, POP2107

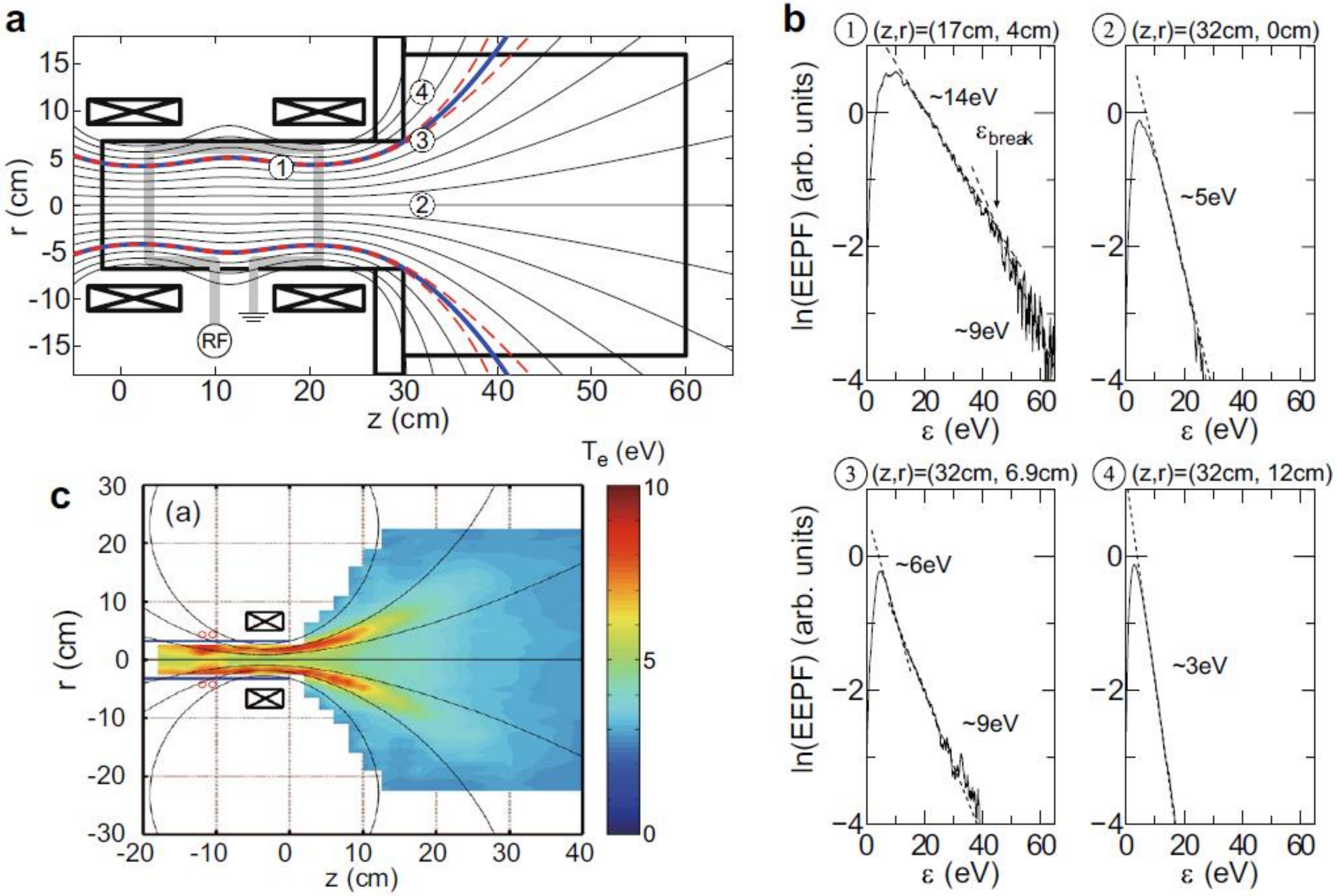

High T_e electrons are generated in the source.
The electrons are tied to the field lines.

Thrust

$F = M = (nk_BT + mnv^2)*A$

Plasma diagnoses

Langmuir probes ---> Plasma density (n), Plasma potential (Vp), Electron temperature (Te)
Retarding field energy analyzer ---> Ion energy distribution (Beam energy, $mv^2/2$)
Laser induced fluorescence ---> Ion and neutral velocities (v)
Optical emission spectroscopy ---> Ion and neutral velocities (v_i, v_n) and temperature (T_i, T_n)

It is not easy to get the absolute values of the density, temperature, and velocity…

Thrust assessment

Thrust balance ---> Absolute value of the force exerted to the thruster
Target balance ---> Absolute value of the force exerted to the target

Takahashi RSI2015

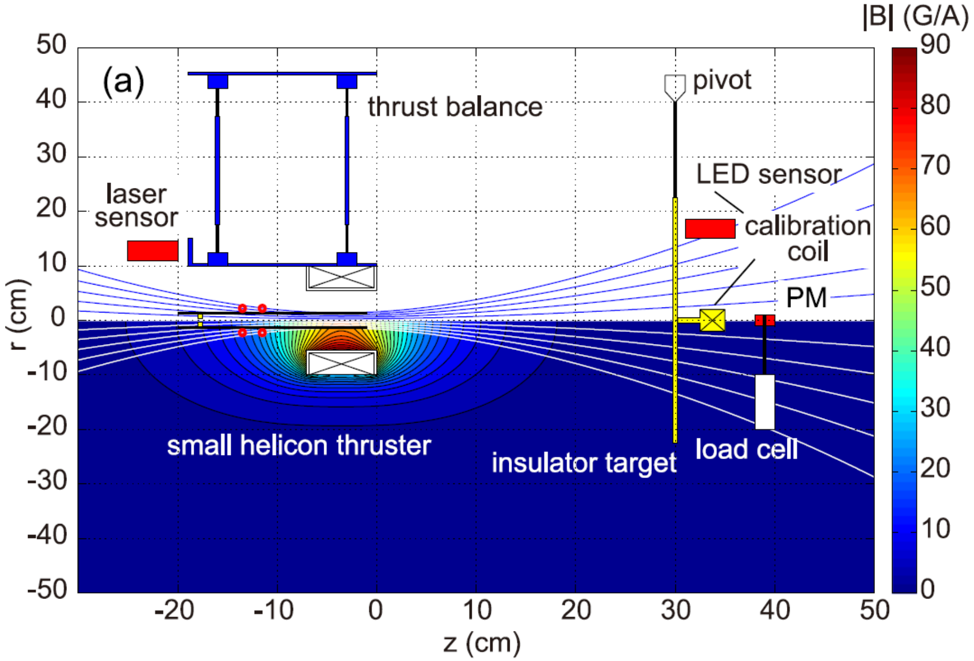

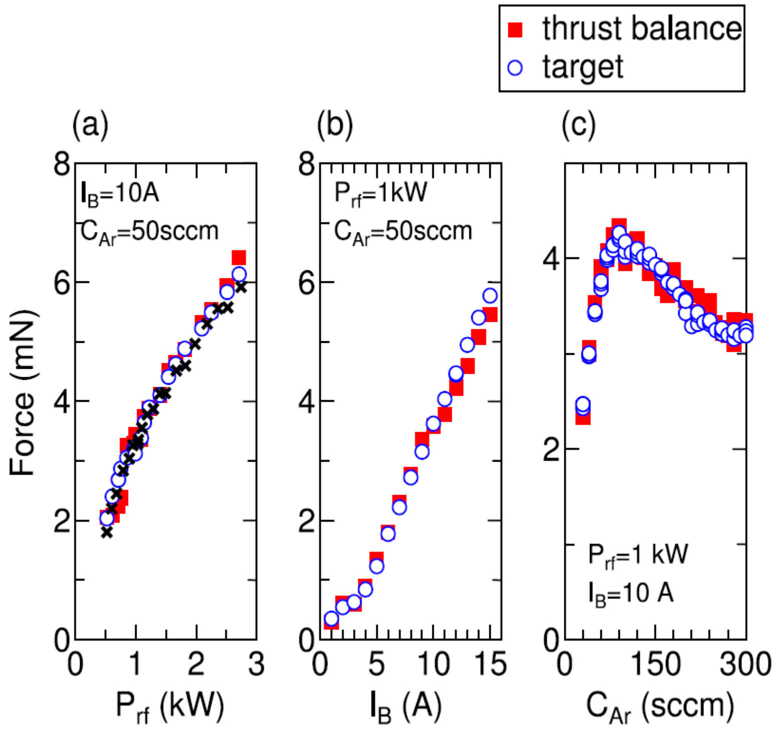

The first direct thrust measurements

Performed in Surry University

Pottinger et al., JPD 2011

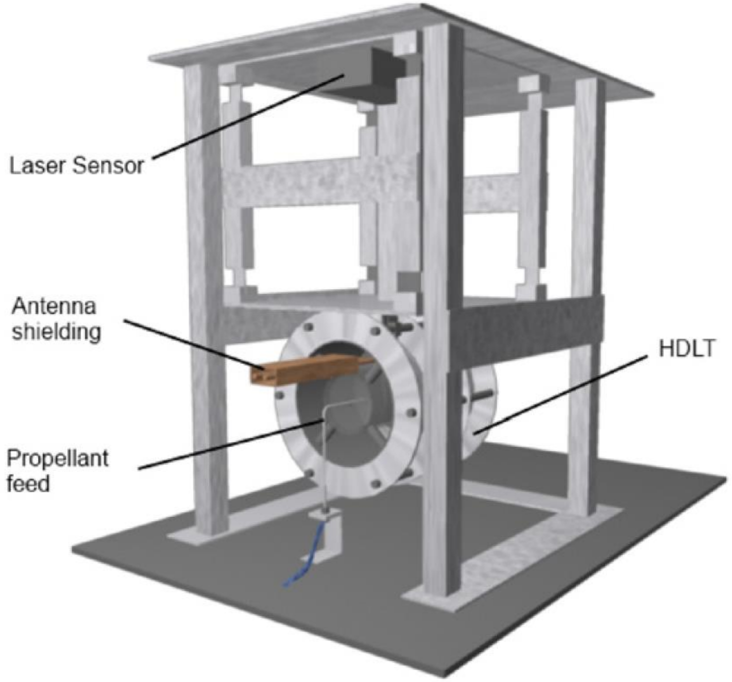

F = 2.8 mN (P_{rf} = 650 W)@Kr
F/P = 4.3 mN/kW
I_{sp} = 286 sec
Efficiency = 0.6 %

Performed in the Australian National University

Takahashi et al., APL 2011

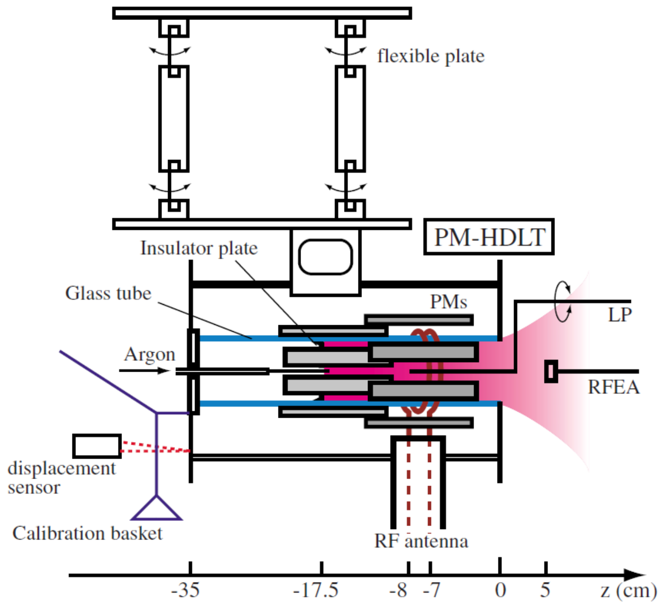

F = 3.3 mN (P_{rf} ~ 0.9kW)@Ar
F/P = 3.7 mN/kW
I_{sp} = 510 sec
Efficiency = 0.8 %

Thrust model with no B field

1-D Momentum equation (negligible electron inertia, $T_i \sim 0$, no B field)

Electron: $-eE_z = \frac{d}{dz}(p_e)$

Ion: $eE_z = \frac{d}{dz}(mnu_z^2)$

$$\frac{d}{dz}(p_e + mnu_z^2) = 0$$

total momentum for unit cross section (momentum flux)

Total thrust for radially uniform plasma = $(p_e + mnu_z^2)$*A

$$\frac{dT}{dz} = \frac{d}{dz}(p_e + mnu_z^2)A = 0$$

Thrust is conserved along z with no B field

Fruchtman PRL2006
Lafleur et al, POP2011

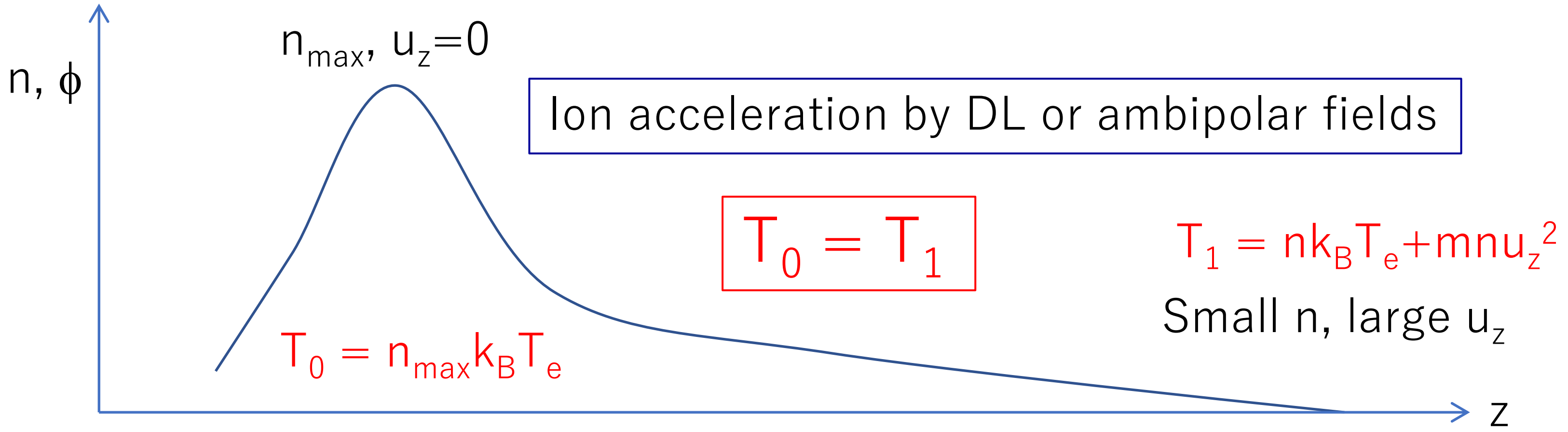

Thrust is given by the electron pressure at the maximum pressure position

Thrust model with the MN

$$m_j \nabla \cdot (n_j \mathbf{v}_j \mathbf{v}_j) = q_j n_j (\mathbf{E} + \mathbf{v}_j \times \mathbf{B}) - \nabla \cdot \mathbf{P}_j$$

Integrated momentum flux (Thrust)

$$T(z) = \iint (p_e + mnu_z^2) d\theta dr$$

$$T_{total}(z) = \boxed{2\pi \int_0^{r_s} r p_e(r, z_0) dr} \quad T_s$$

$$\boxed{-2\pi \int_{z_0}^{z} \int_0^{r_p(z)} r \frac{B_r}{B_z} \frac{\partial p_e}{\partial r} drdz} \quad T_B$$

$$\boxed{-2\pi \int_{z_0}^{z} \int_0^{r_p(z)} \frac{\partial}{\partial r} (rmnu_r u_z) drdz,} \quad T_w$$

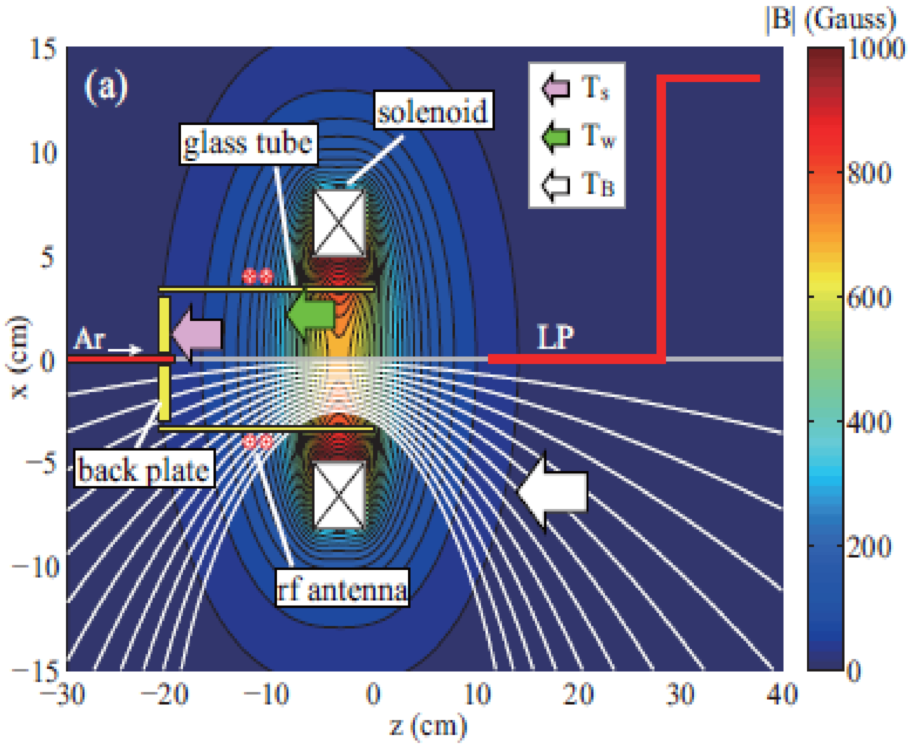

Takahashi et al., PRL 2011a

* j_θ is the electron diamagnetic current.

* ExB drift current (Hall current) is neglected for the fully magnetized model.

Individual thrust measurements

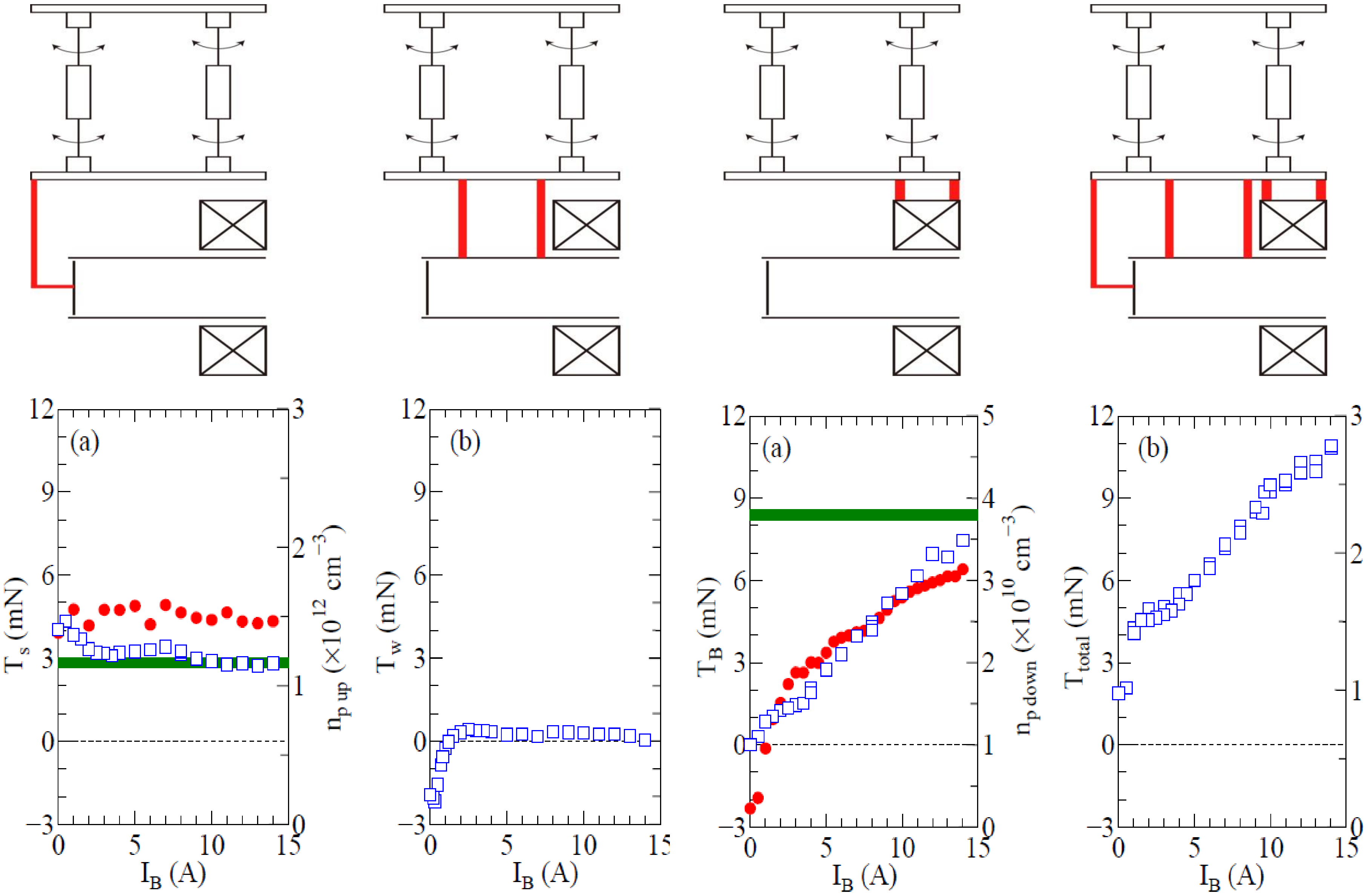

Takahashi et al., PRL 2013

Internal plasma current inducing T_B

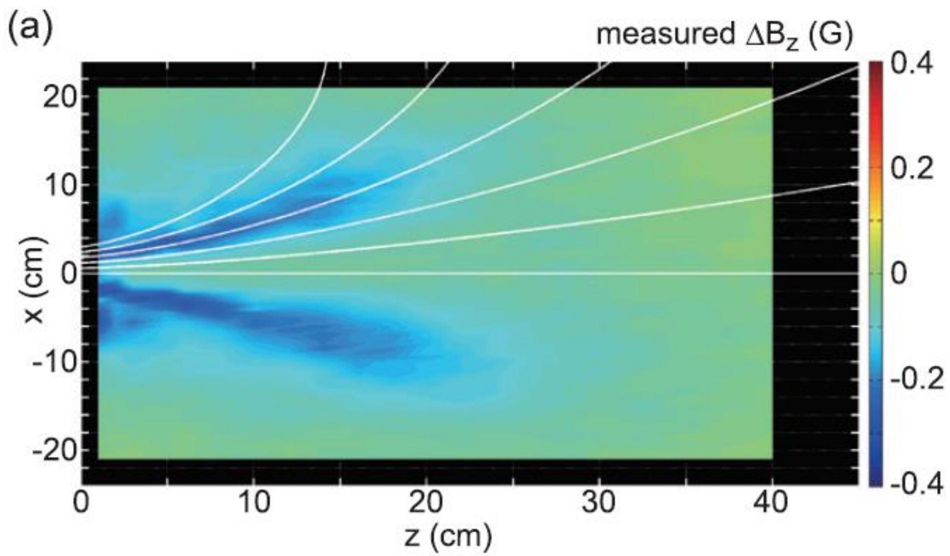

$$j_\theta = -\frac{1}{\mu_0}\frac{\partial \Delta B_z}{\partial r} + \frac{1}{\mu_0}\frac{\partial \Delta B_r}{\partial z}$$

$$\sim -\frac{1}{\mu_0}\frac{\partial \Delta B_z}{\partial r}$$

$$\boxed{J_\theta = J_{De} + J_{ExB}}$$

$$J_{De} >> J_{ExB}$$

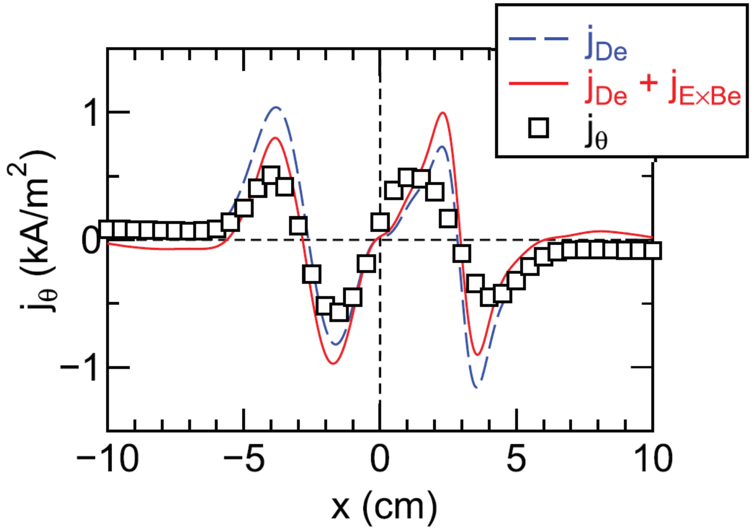

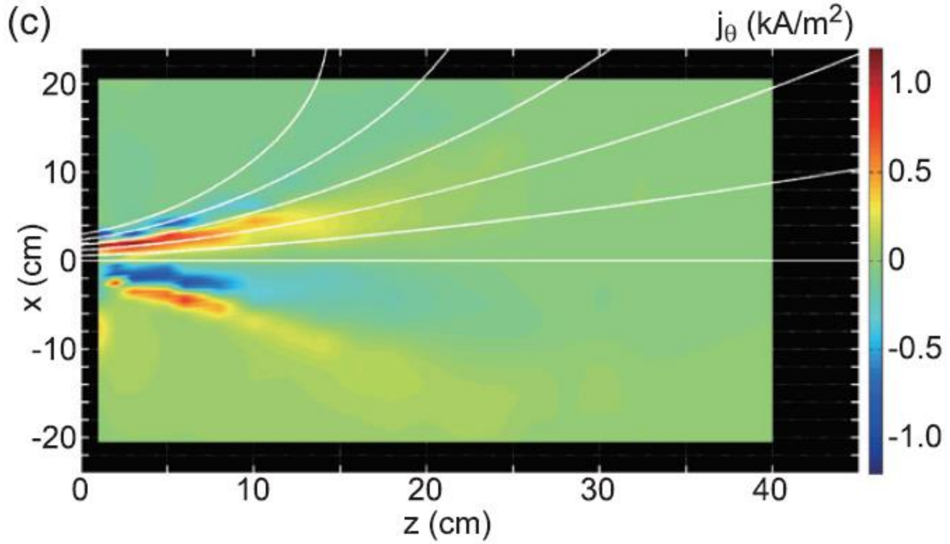

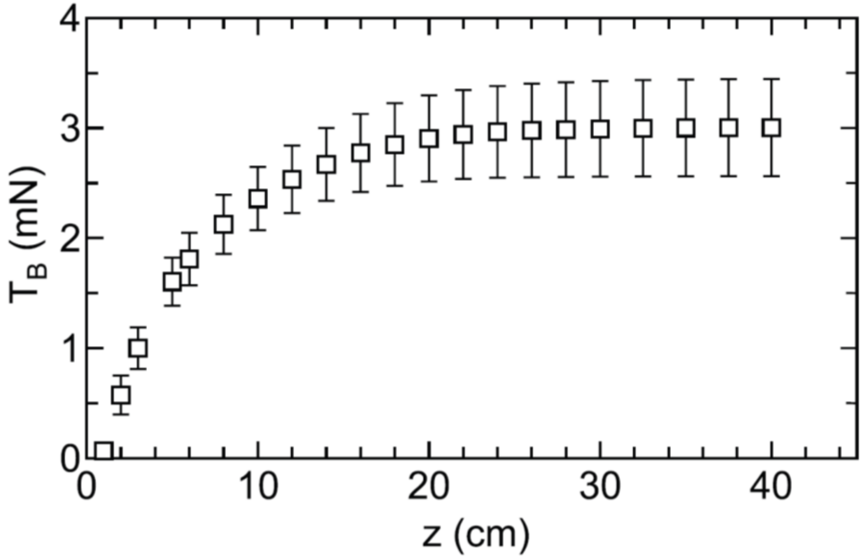

Takahashi et al., PSST 2016

Lorentz force integrated from the source exit (z=0).

Axial momentum lost to the radial wall (T_W)

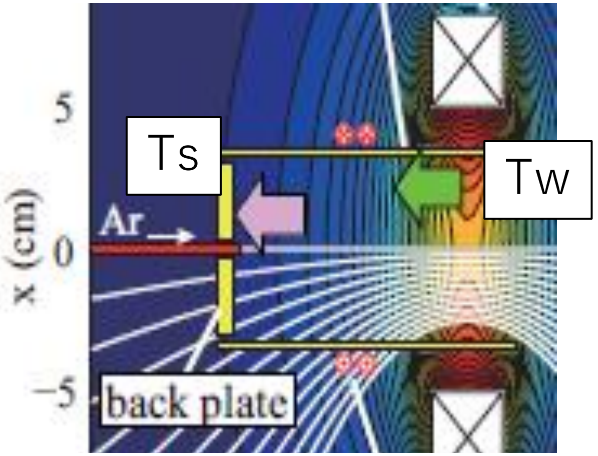

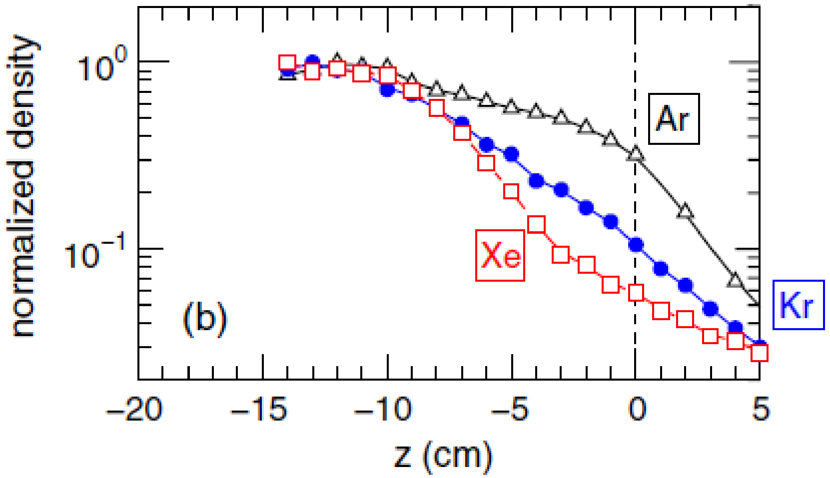

Prf = 1 kW
m_{dot} = 0.75 mg/s
Ionization rate Xe > Kr > Ar

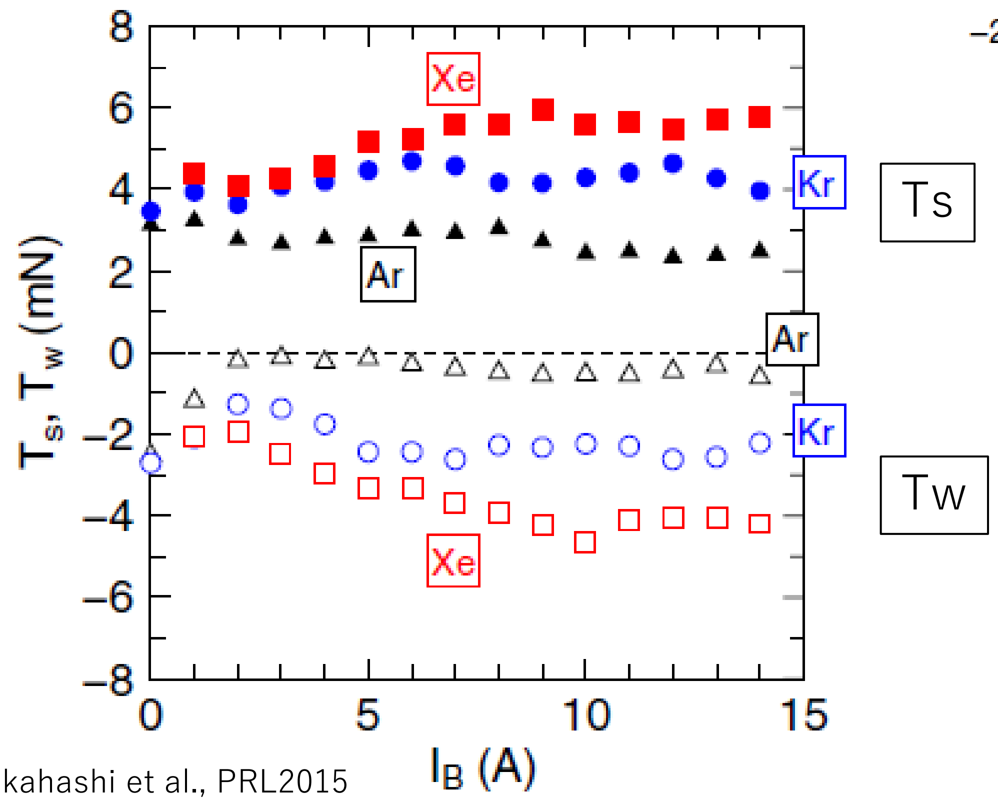

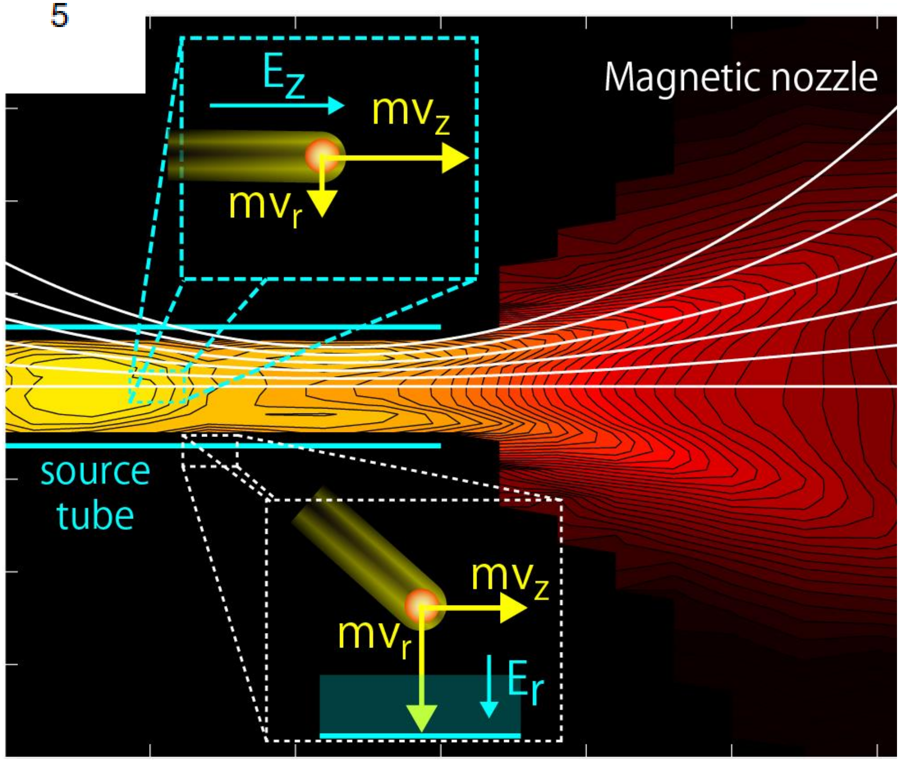

Takahashi et al., PRL2015

Density profile due to neutral depletion

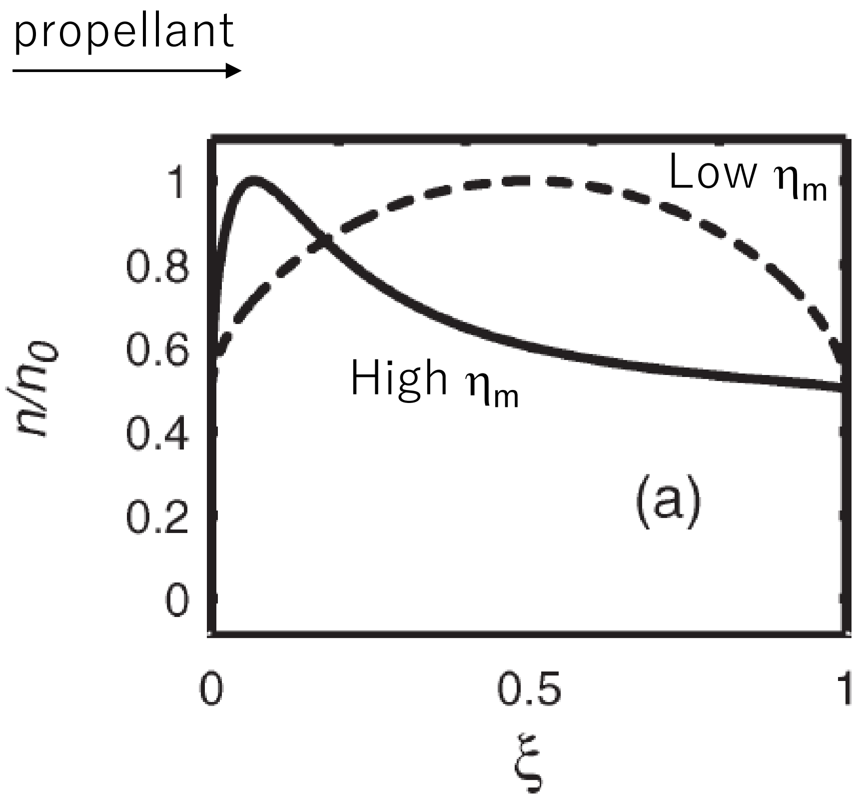

η_m: propellant utilization efficiency

Prf = 5kW

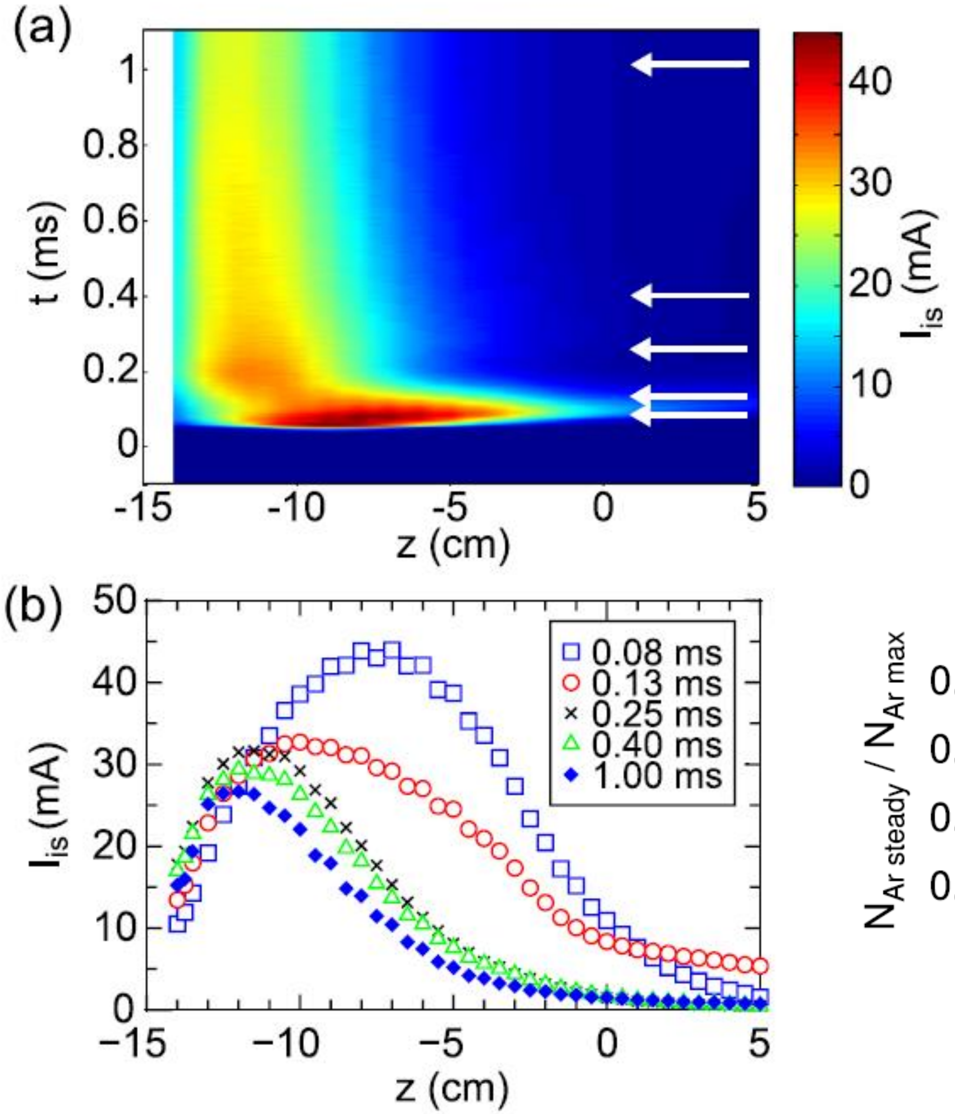

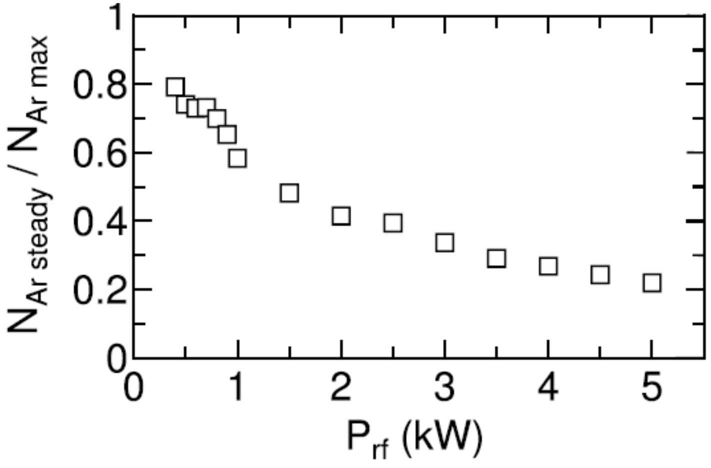

Fruchtman IEEE 2008

Takahashi et al., APL2016a

Gas injection affects the profile and the thruster performance

65-mm-diameter source

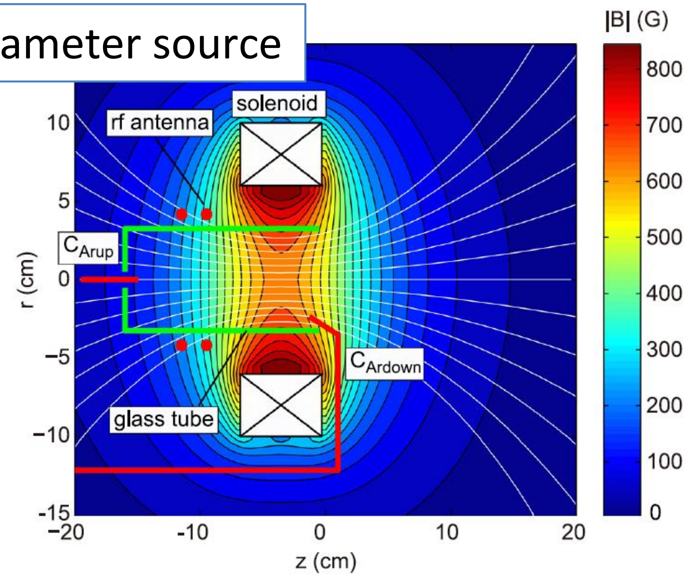

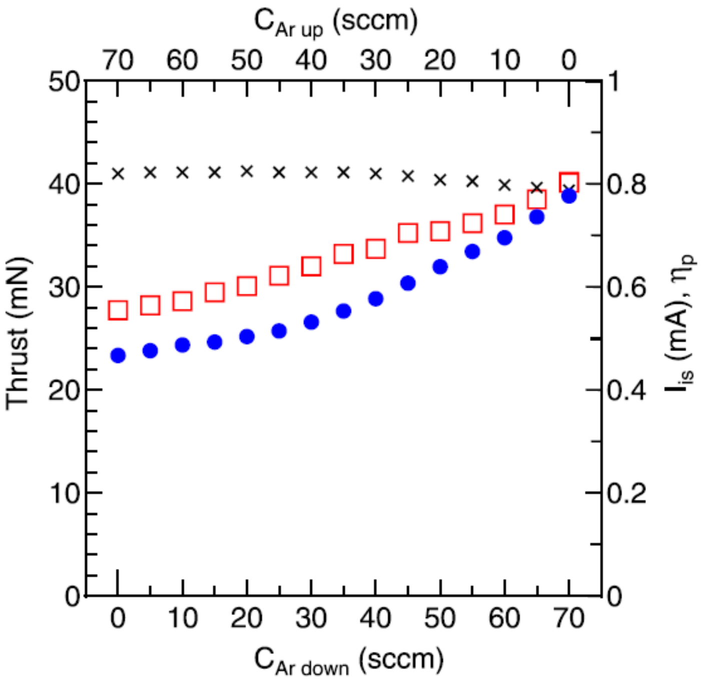

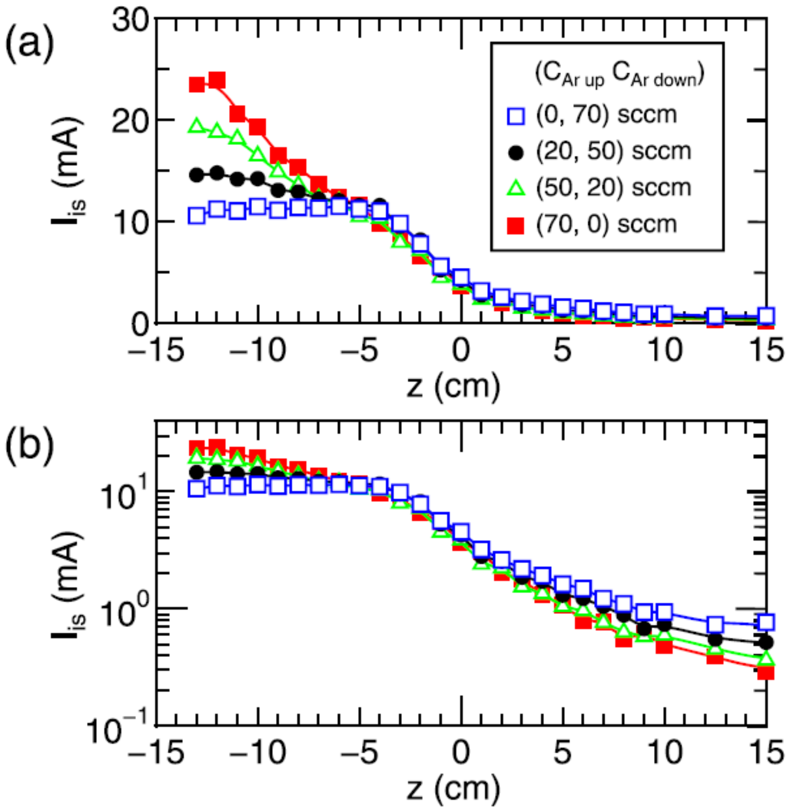

Takahashi et al., APL2016b

Thruster model combining the global source model and the 1-D MN model

Global model inside the source

Assuming

- No radial loss of the axial momentum (T_w)
- No magnetic field inside the source
- M = 1 velocity at the open source exit

Particle balance $K_{iz}n_0n_gV = n_0u_BA_{eff},$

Power balance $P_{abs} = en_0A_{eff}u_BE_T,$

$$A_{eff} = 2\pi RLh_R + 2\pi R^2h_L$$

Neutral density $m_{dot} = M_nn_gv_gA_s$

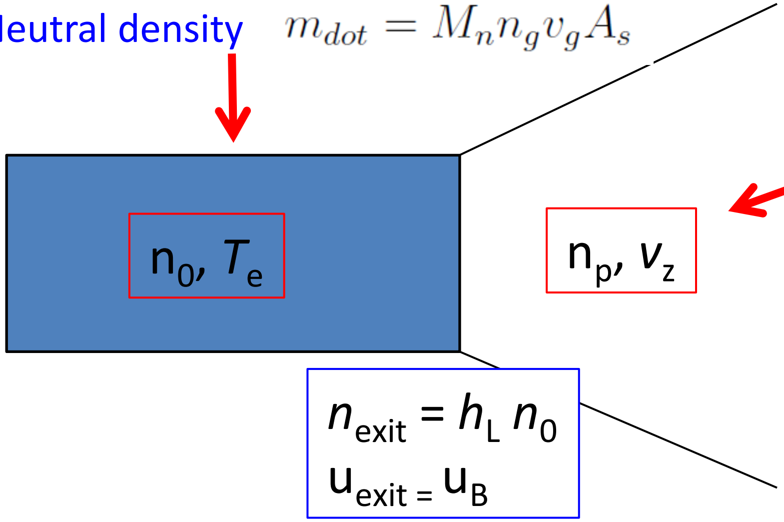

One-dimensional magnetic nozzle model

Assuming

- Isothermal electron temperature
- Magnetized plasma expansion
- No radial loss from the magnetic nozzle (n*v*A = constant)

Thrust model $T_{total}(z) = T_s + T_B,$ Fruchtman et al., POP2012

$$T_s = n_0k_BT_eA_s,$$

$$T_B = -\int_0^z \frac{n_pk_BT_eA}{B_z}\frac{\partial B_z}{\partial z'}dz',$$

Plasma expansion along the magnetic flux tube

$$B_{zi}A_s = B_zA = constant$$

Flow velocity $\frac{M^2 - M_i^2}{2} - \ln\left(\frac{M}{M_i}\right) = \ln\left(\frac{B_{zi}}{B_z}\right),$

Flux conservation $n_pMu_BA = n_{exit}u_BA_s$

Lieberman and Lichtenberg, Principles of plasma discharges and material processing

Effect of the source diameter

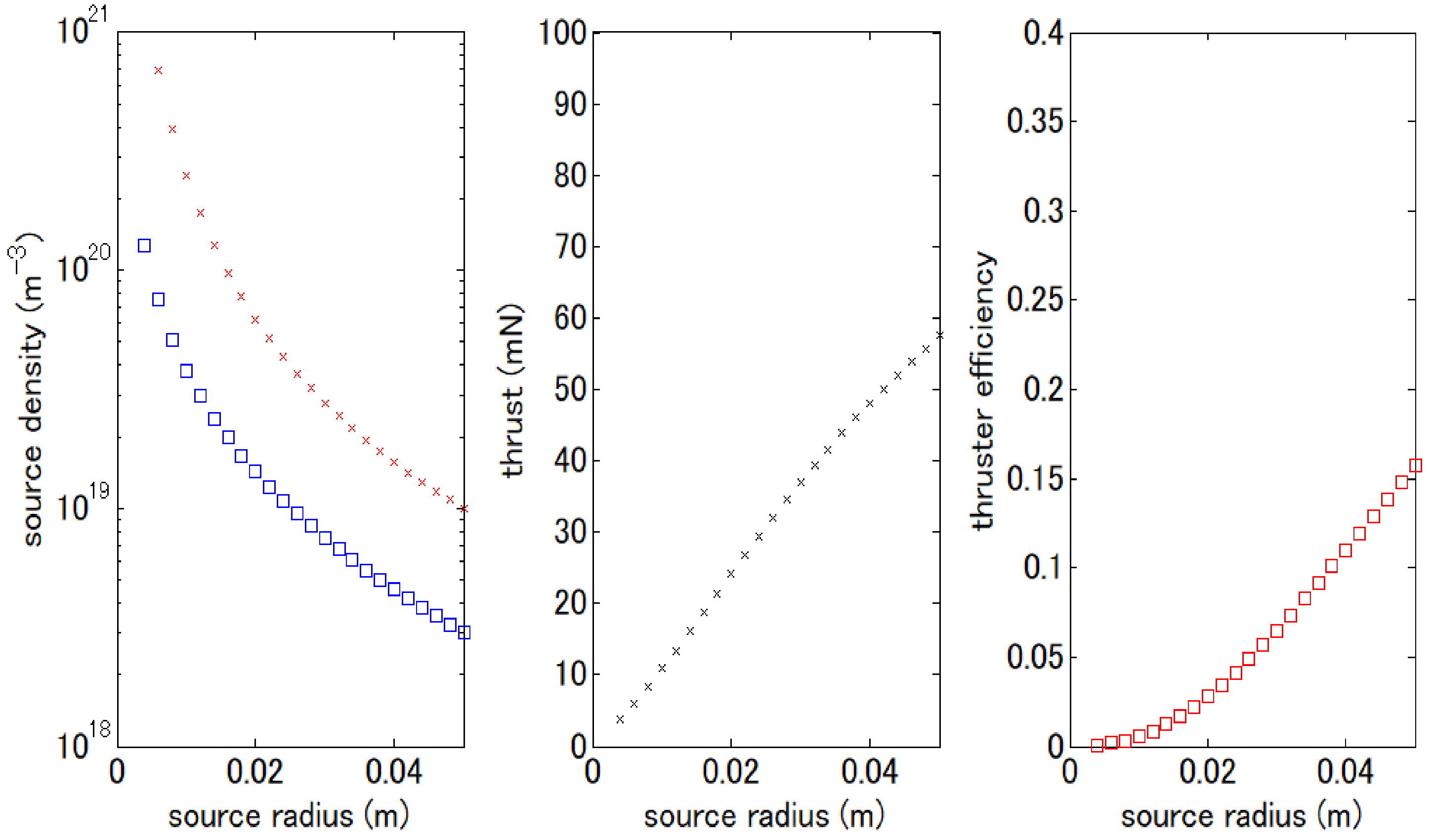

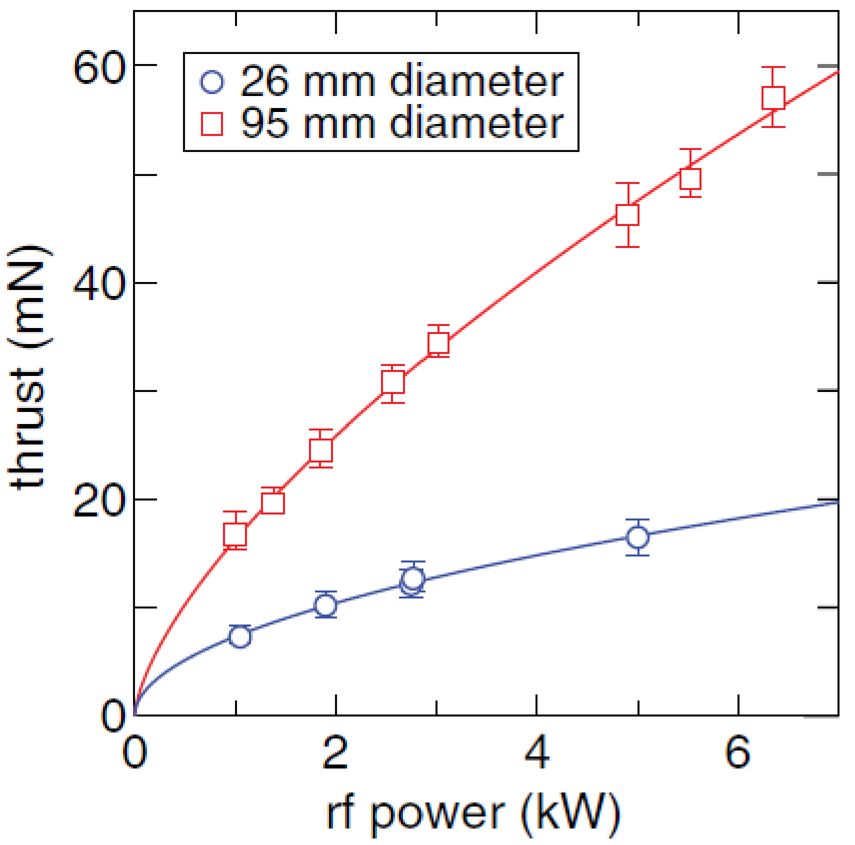

P_{rf} = 5 kW
C_{Ar} = 2.1 mg/s
L = 17.5 cm

$\eta_T = F^2 / (2\ m_{dot}\ P_{rf})$

Takahashi et al., PSST2015

How can we improve the performance?

1- Strong magnetic field (Electron diamagnetic thrust, T_B)

2- Large diameter source cavity (Particle and power balances)

3- Downstream gas injection (Density profile)

95-mm-diameter source

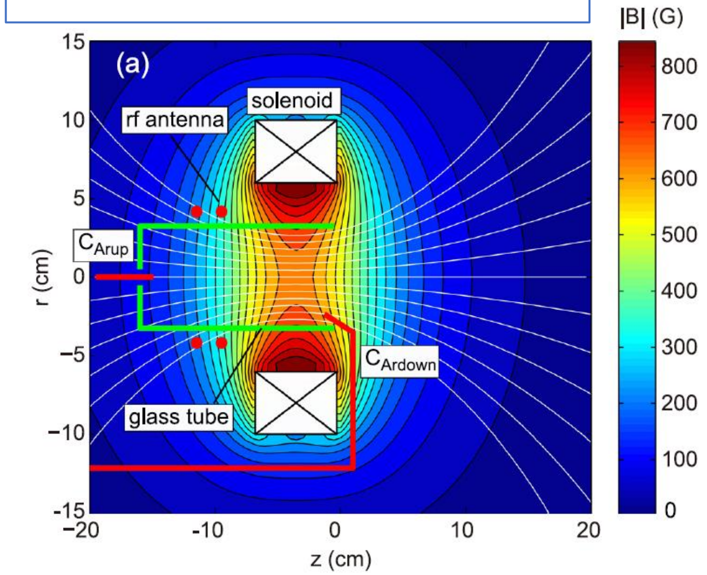

95-mm-diameter source tube
Downstream gas injection
Strong magnetic field

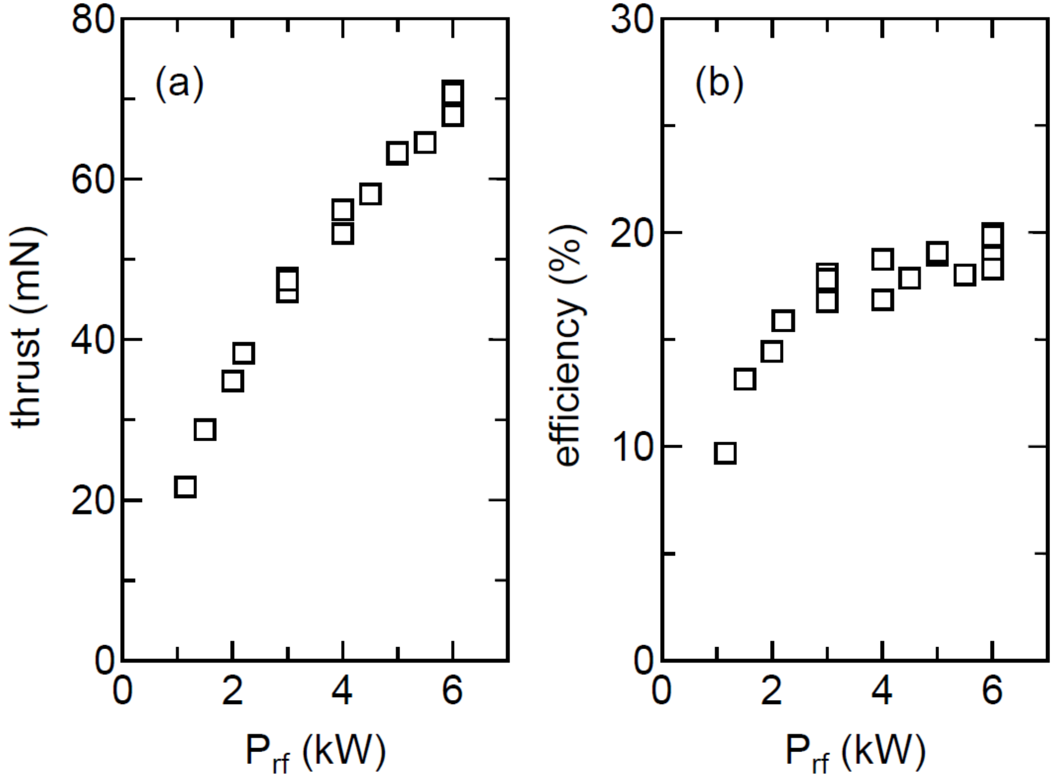

Takahashi, Sci Rep 2021

Thruster performance assessment

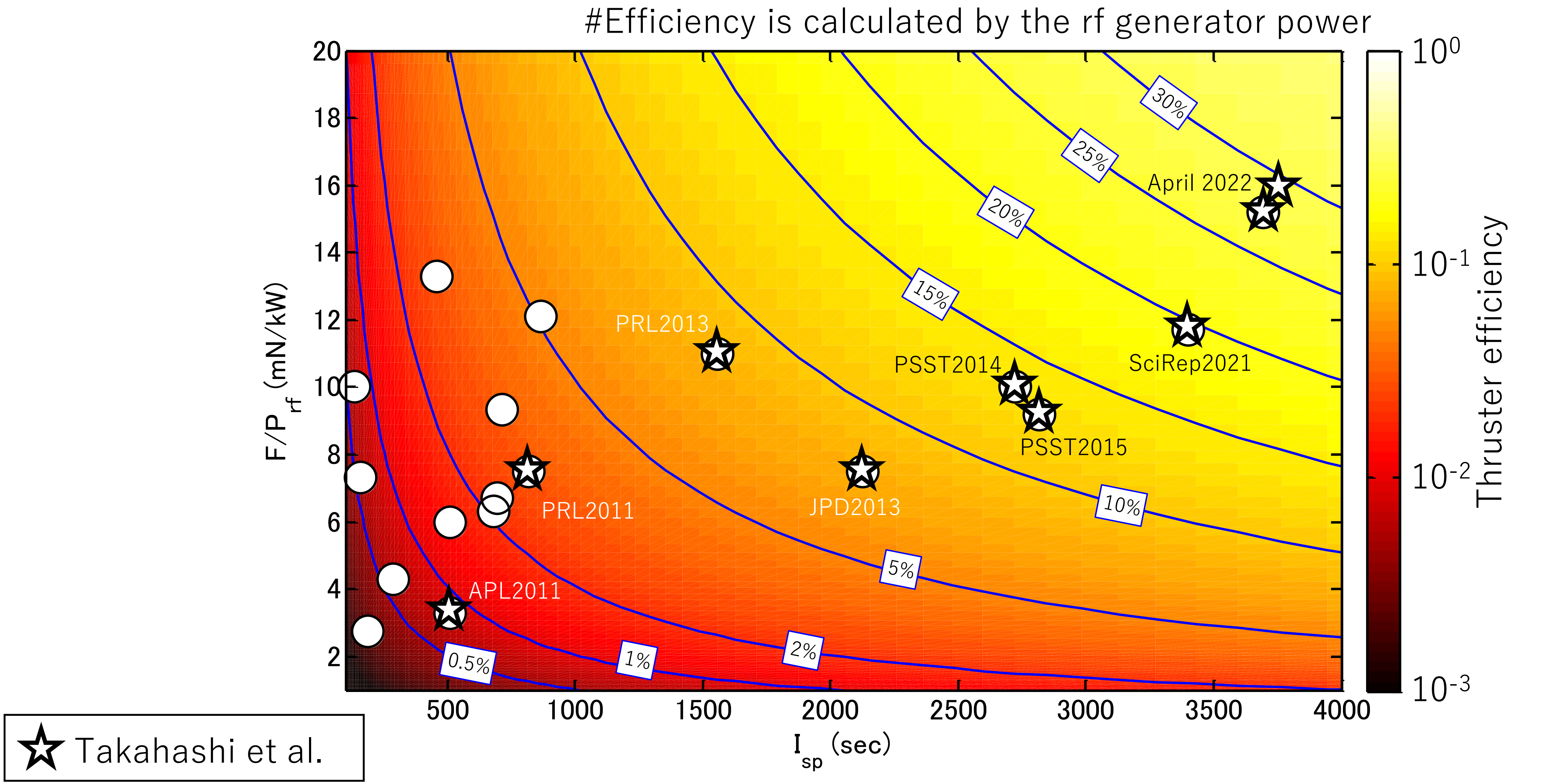

Thruster efficiency is further increased in April 2022 experiments (Kazu's Mega-HPT Labbook Vol6, page 430-431)

Plasma detachment

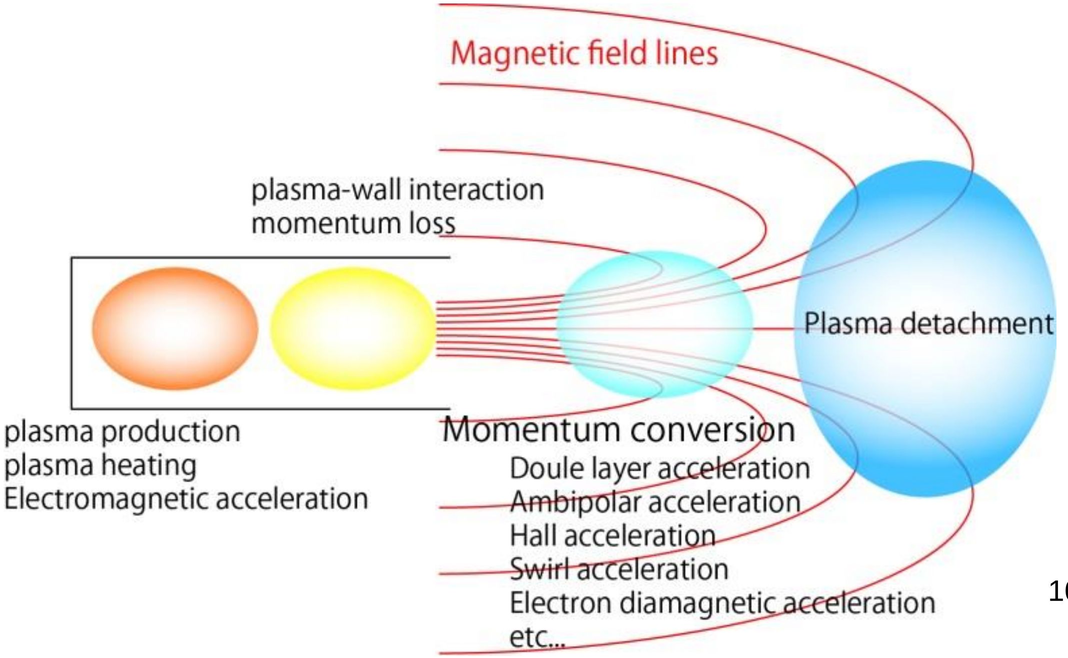

Electrons are still magnetized

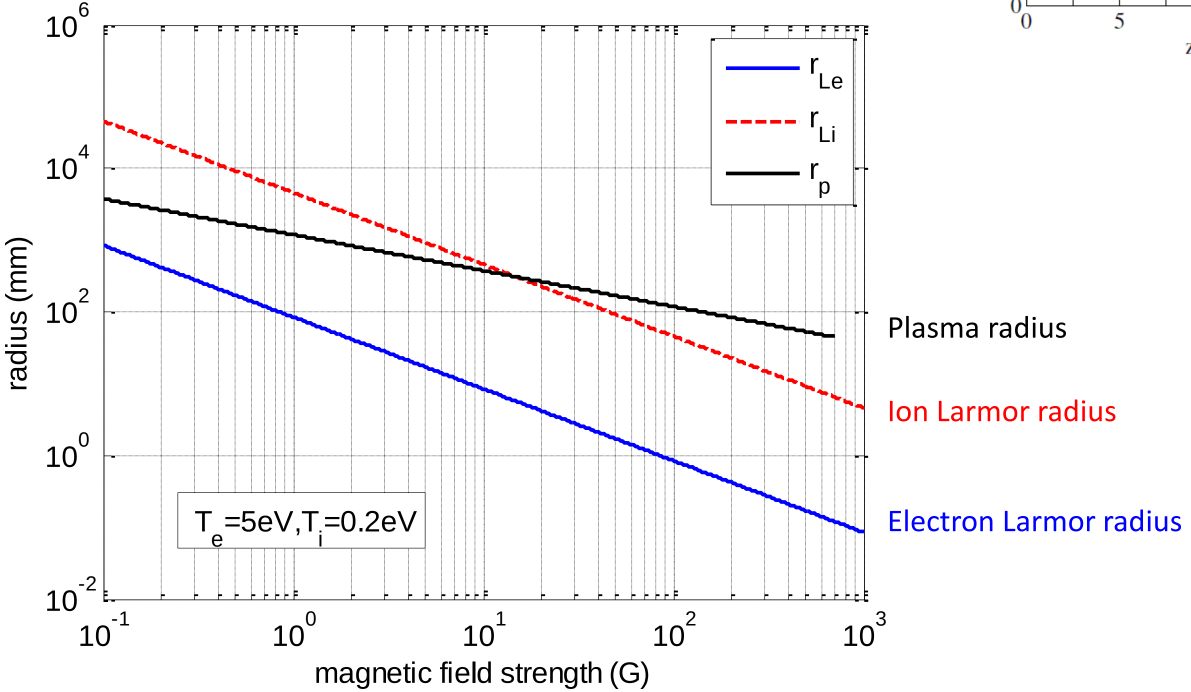

Ion detachment (demagnetization)

Cox et al., APL2008

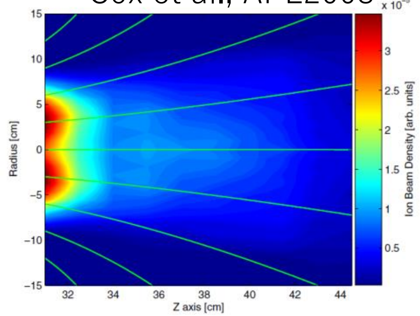

Charles et al, PRL2009

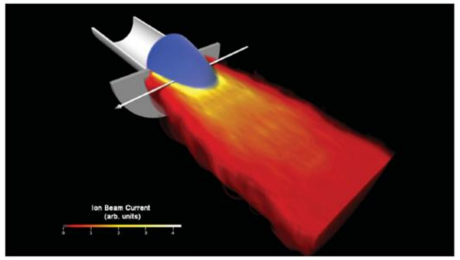

Takahashi et al., JPD2011

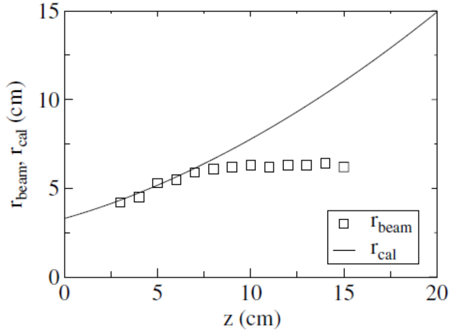

MHD detachment scenario

PHYSICS OF PLASMAS **12**, 043504 (2005)

Magnetohydrodynamic scenario of plasma detachment in a magnetic nozzle

Alexey V. Arefiev and Boris N. Breizman
Institute for Fusion Studies, The University of Texas, Austin, Texas 78712

(Received 22 July 2004; accepted 20 January 2005; published online 25 March 2005)

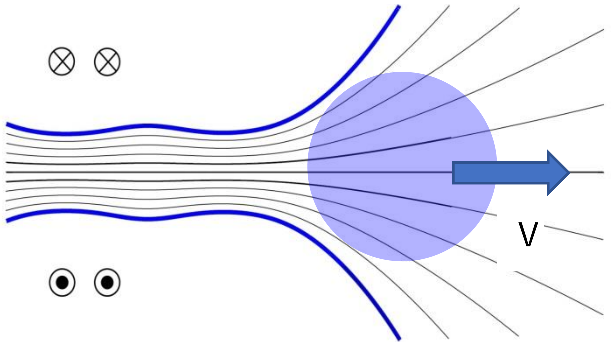

Their analysis concludes
A plasma flow can detach from a spacecraft together with the field lines that become stretched along the flow. This is actually occurring around the Sun and the solar wind sometimes take their magnetic field to our Earth.

This can occur when the plasma flow energy overcomes the magnetic field energy, corresponding to the case *of super Alfvénic flow ($M_A = v/v_A > 1$)*

$$\frac{1}{2}mnv^2 > \frac{B^2}{2\mu} \Rightarrow v > \frac{B}{\sqrt{\mu mn}} = v_A$$

What should we measure to verify the stretch?

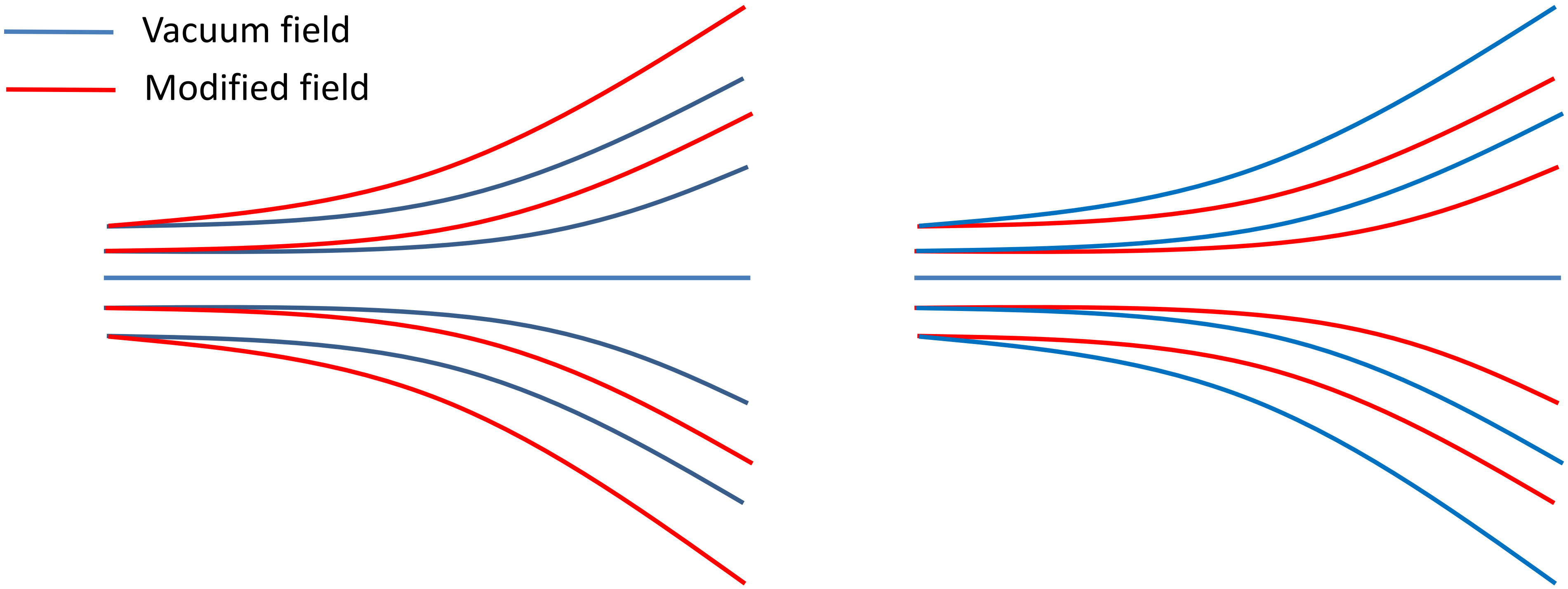

Diverged case

Negative ΔB_z

Stretched case

Positive ΔB_z

The first observation of the MN stretch

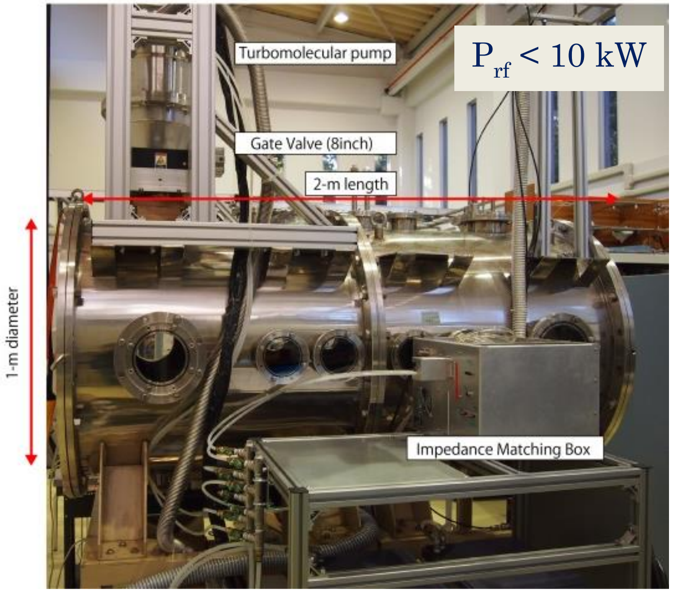

PRL **118,** 225002 (2017) PHYSICAL REVIEW LETTERS week ending 2 JUNE 2017

Laboratory Observation of a Plasma-Flow-State Transition from Diverging to Stretching a Magnetic Nozzle

Kazunori Takahashi* and Akira Ando
Department of Electrical Engineering, Tohoku University, Sendai 980-8579, Japan

(Received 20 February 2017; revised manuscript received 18 April 2017; published 2 June 2017)

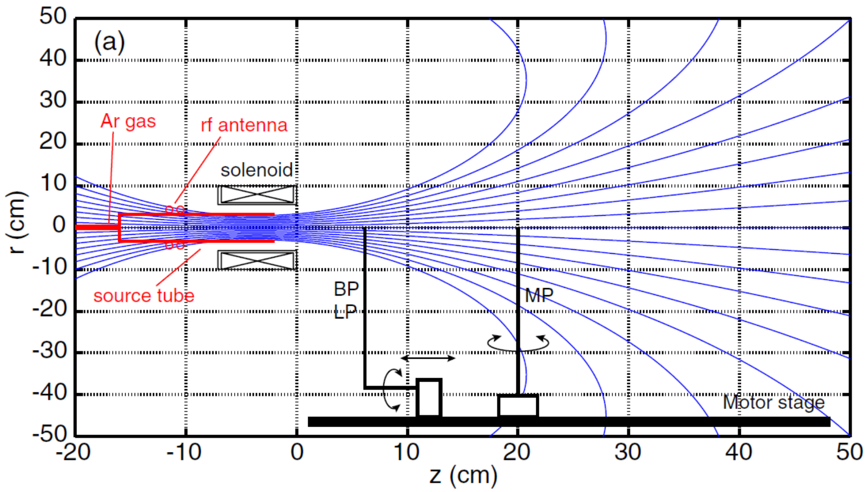

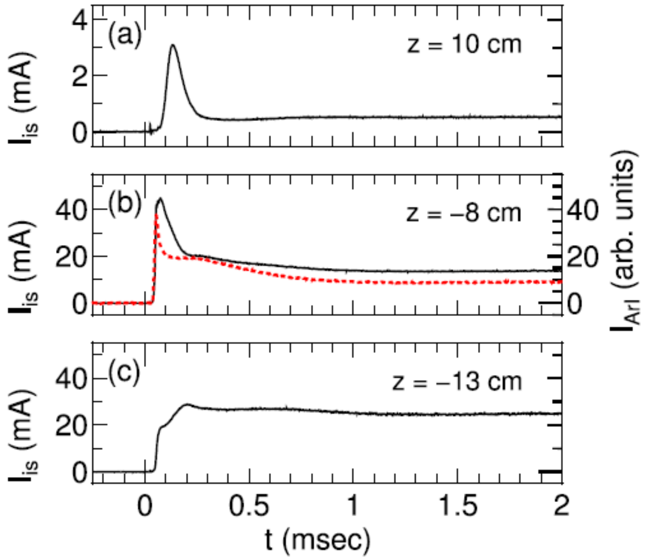

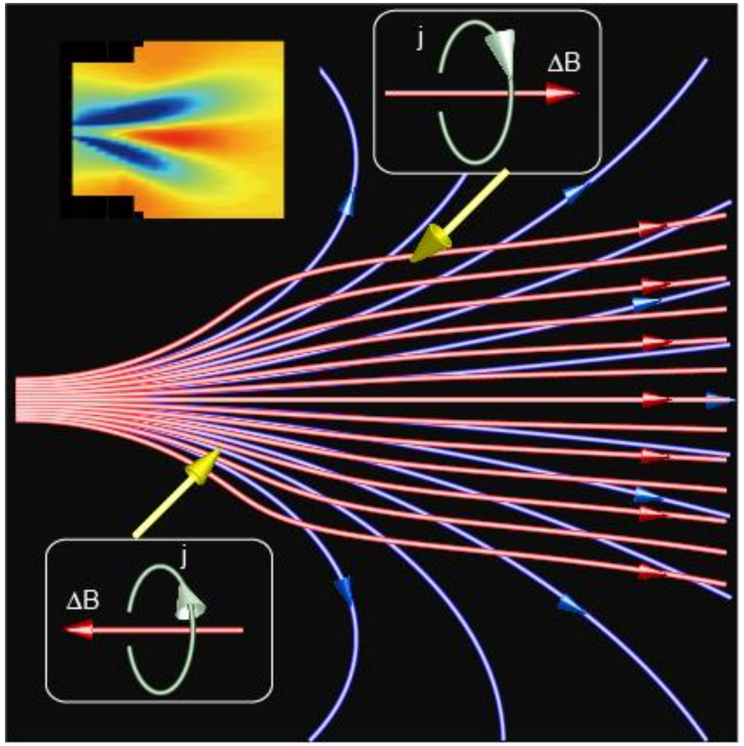

Measurement of the plasma-induced magnetic field ΔB_z

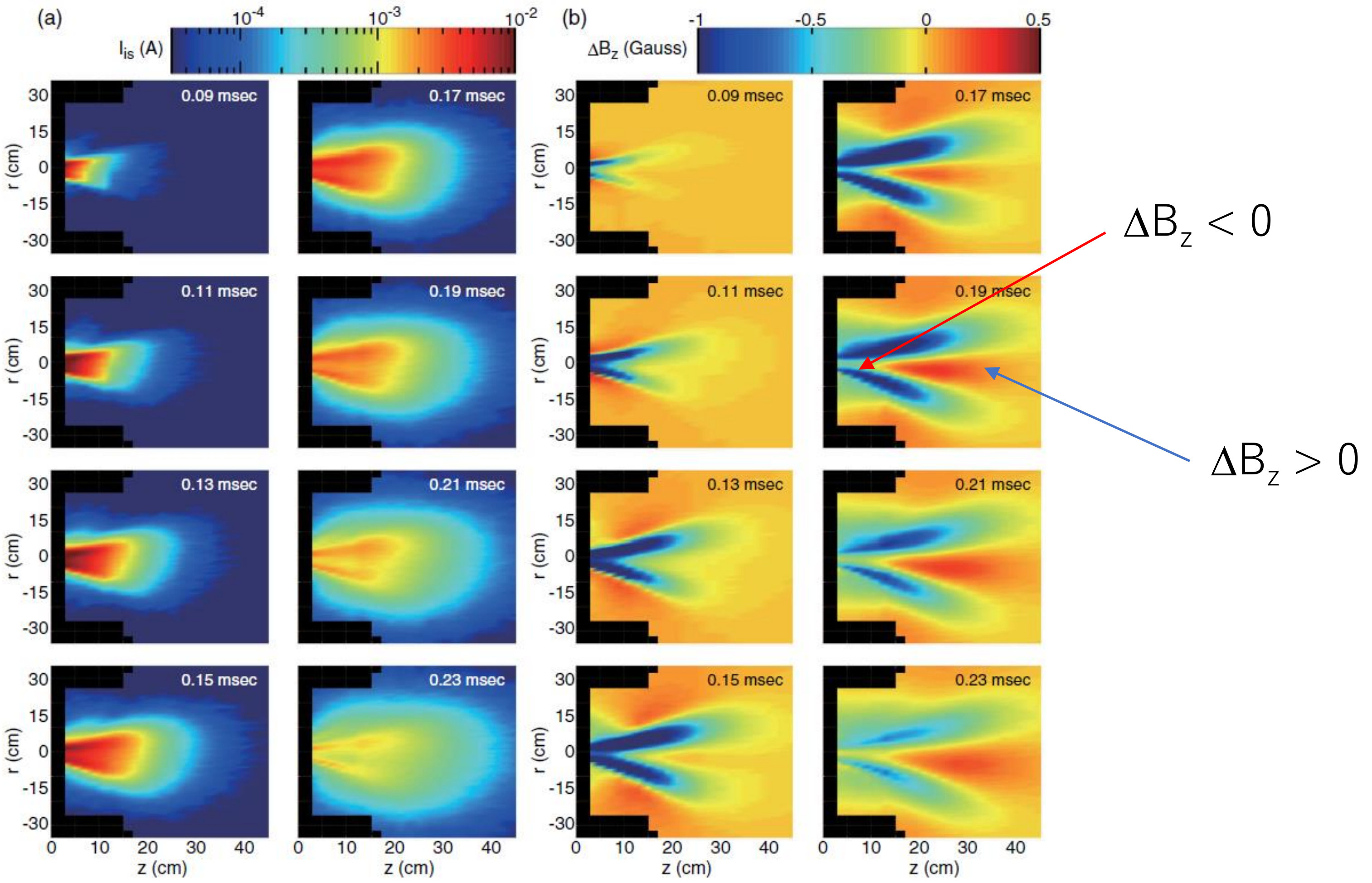

FIG. 2. Spatiotemporal evolution of (a) I_{is} and (b) ΔB_z, taken for $I_B = 4.5$ A and $P_{rf} = 5$ kW. The rf power is triggered at $t = 0$ and the signals are averaged over 16 shots, where the measurements are performed at ~1200 points (~20 points along z and ~60 points along r). A movie can also be found as Supplemental Material [29].

Where does the stretch occur?

V = Mi*Cs ~ 2 km/s

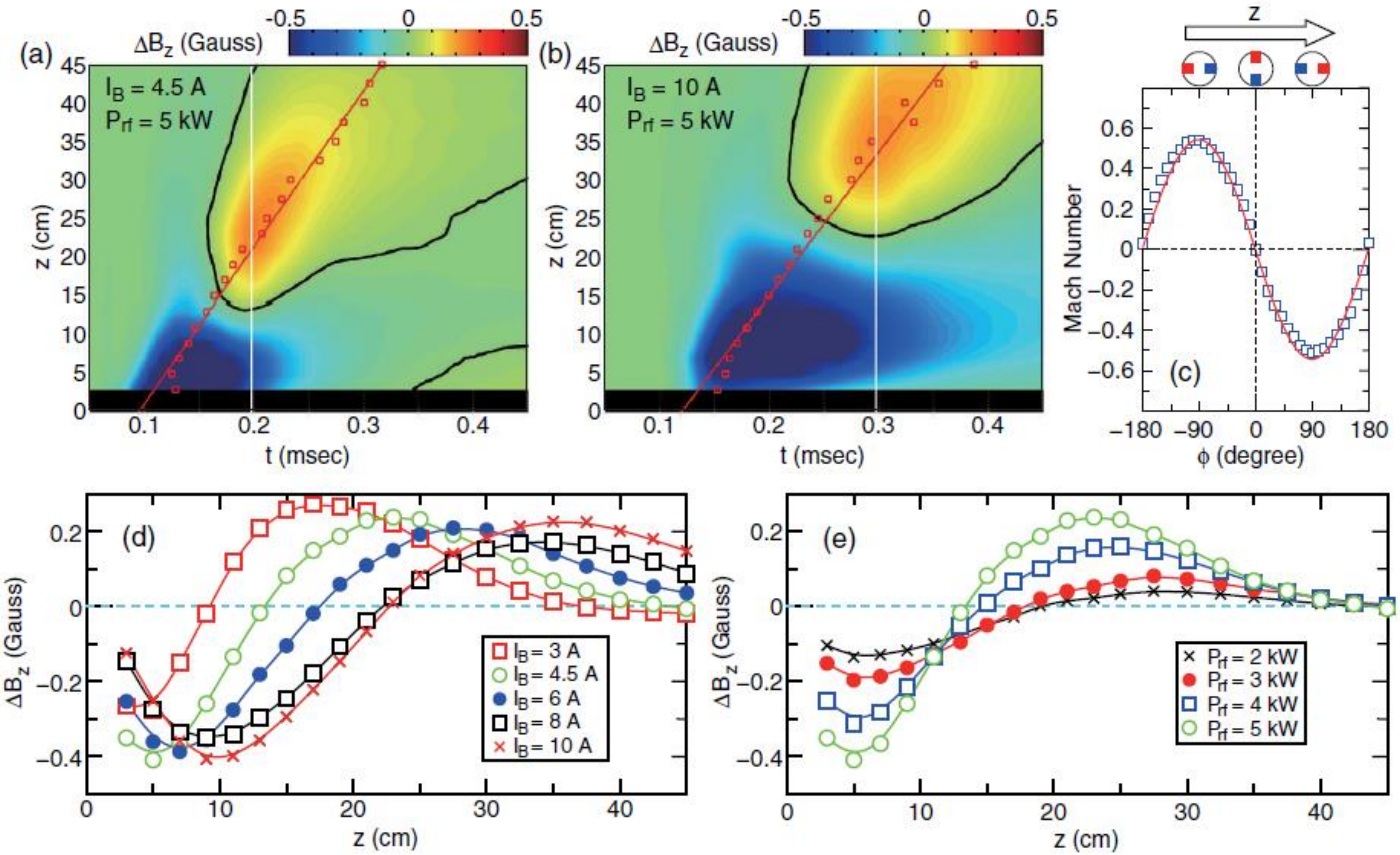

What parameter decides the stretch ?

Generally, the stretch occurs for the super Alfvénic flow ($M_A = v/v_A > 1$)

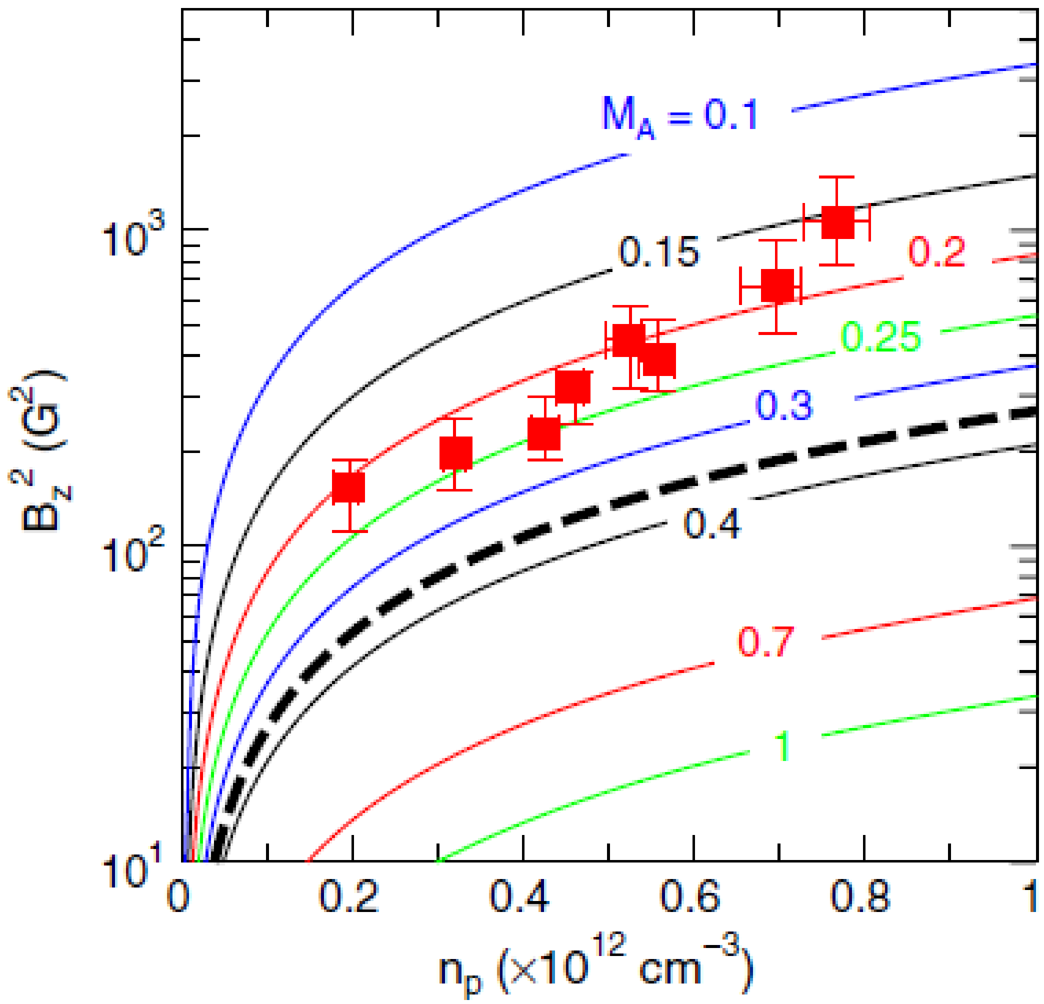

FIG. 4. Measured plasma density n_p and the square of the applied magnetic field strength B_z at the transition positions. The solid lines and the bold dashed line correspond to Eq. (1) for various values of the Alfvén Mach number M_A and Eq. (3), respectively, where the measured values of $v = 2$ km/s and $T_e = 5$ eV are used for the calculation.

The experiment shows that the stretch starts to occur at the lower Alfvén Mach Number than unity.

Force balance in an ideal MHD approximation (1)

Inertia term

Magnetic pressure force

$$\rho(\mathbf{v}\cdot\nabla)\mathbf{v} = -\nabla p - \frac{\nabla B^2}{2\mu} + \frac{(\mathbf{B}\cdot\nabla)\mathbf{B}}{\mu},$$

Pressure force

Magnetic tension

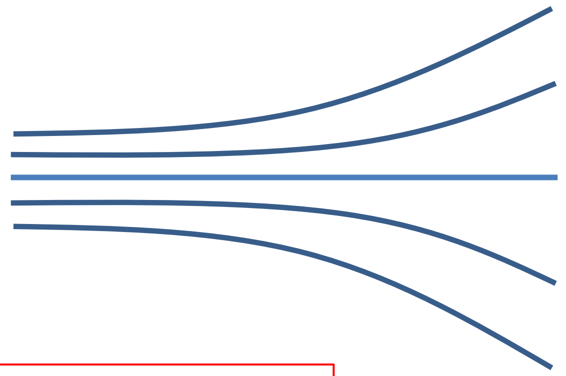

$\boxed{\text{Upstream limit}}$

1- Zero velocity (v ~ 0)
2- Straight axial magnetic field
(negligible tension term)

$$\nabla\left(p + \frac{B^2}{2\mu}\right) = 0,$$

hence $$p + \frac{B^2}{2\mu} = \frac{B^2_{vac}}{2\mu},$$

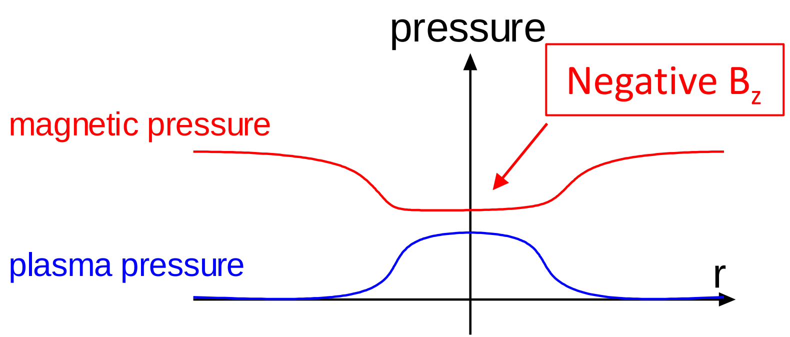

$\boxed{\text{Downstream limit}}$

1- low plasma pressure (p ~ 0)
2- low magnetic field
(negligible magnetic pressure)

$$\rho(\mathbf{v}\cdot\nabla)\mathbf{v} = \frac{(\mathbf{B}\cdot\nabla)\mathbf{B}}{\mu}.$$

$$\left|\frac{\rho v^2}{L}\right| \simeq \left|-\frac{B^2}{\mu L}\right|$$

$$\boxed{v^2 \sim V_A^2 = \frac{(B_{vac}+\Delta B)^2}{mn\mu}}$$

$$\text{For } v > V_{Avac} = \frac{B_{vac}}{\sqrt{mn\mu}}$$

ΔB should be positive to maintain the equilibrium.

Force balance in an ideal MHD approximation (2)

$\boxed{\text{Intermediate condition}}$

$$\rho(\mathbf{v}\cdot\nabla)\mathbf{v} = -\nabla p - \frac{\nabla B^2}{2\mu} + \frac{(\mathbf{B}\cdot\nabla)\mathbf{B}}{\mu},$$

Dimension analysis
($\nabla \rightarrow$ 1/L for velocity
and -1/L for the decreasing B and p)

$$\left|\frac{\rho v^2}{L}\right| \simeq \left|\frac{p_e}{L} + \frac{B^2}{2\mu L} - \frac{B^2}{\mu L}\right|,$$
$$= \left|\frac{nk_BT_e}{L} - \frac{B^2}{2\mu L}\right|.$$

$$\boxed{v^2 \sim \frac{1}{2}V_A^2 - C_s^2 = \frac{1}{2}\frac{(B_{vac}+\Delta B)^2}{mn\mu} - C_s^2}$$

For $v^2 > \frac{1}{2}V_{Avac}^2 - C_s^2 = \frac{1}{2}\frac{B_{vac}^2}{mn\mu} - C_s^2,$

ΔB should be positive to maintain the equilibrium.

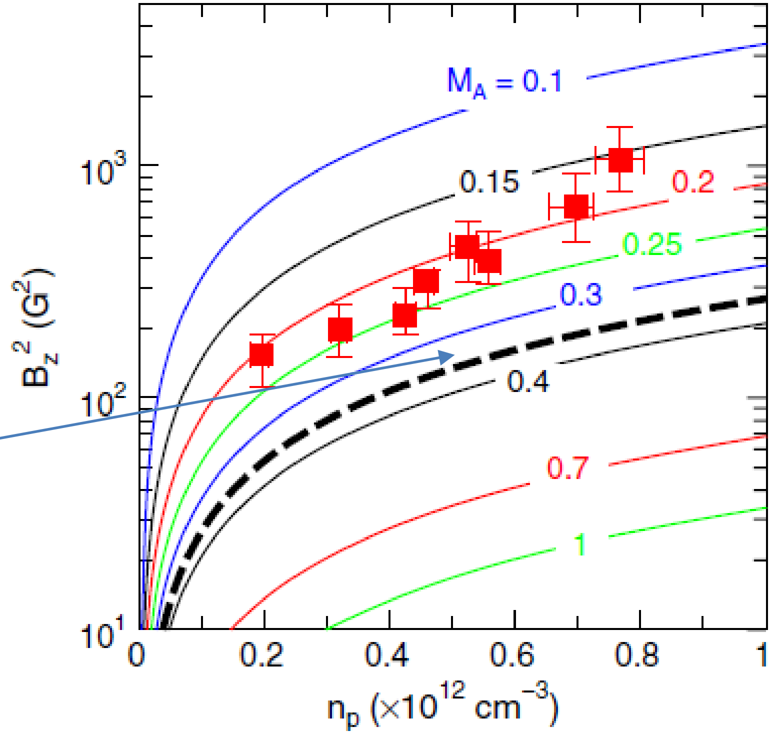

Space debris

Debris are non-cooperative objects (uncontrollable).

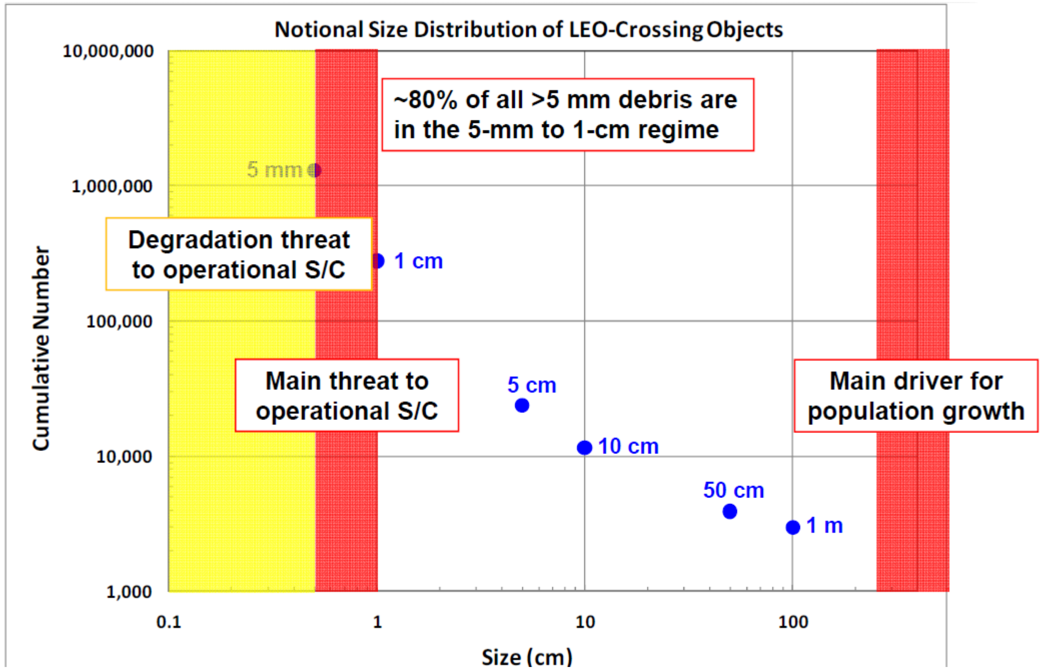

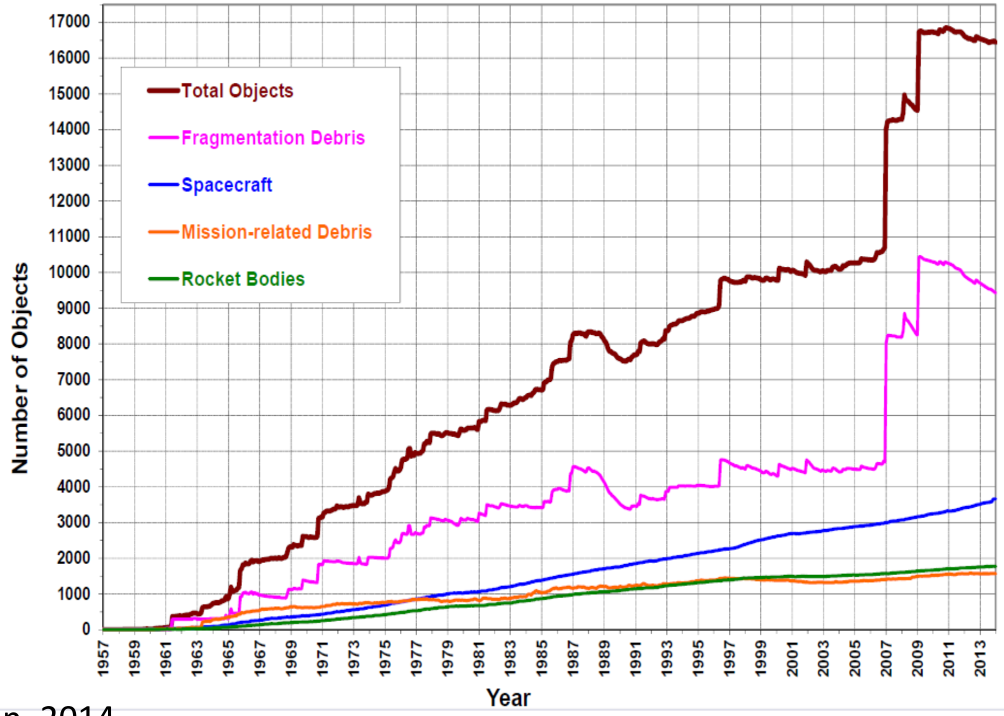

The top priority is removal of large debris;
Typically ~ a ton in weight
a few meter in size

Liou, European Workshop on Space Debris Modeling and Environment Remediation, 2014

Debris removal

Contact removal

Arm capturing

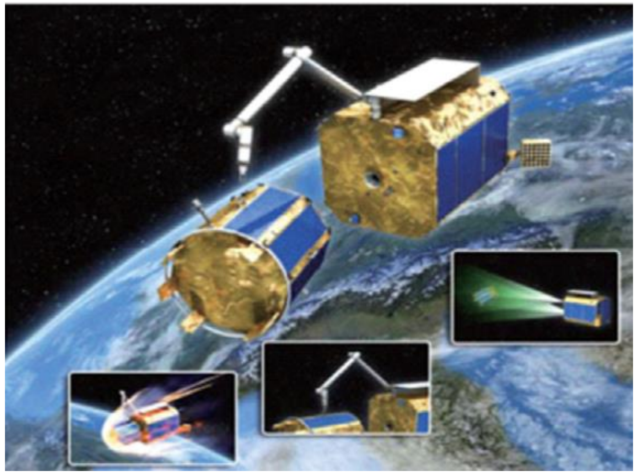

Net capturing

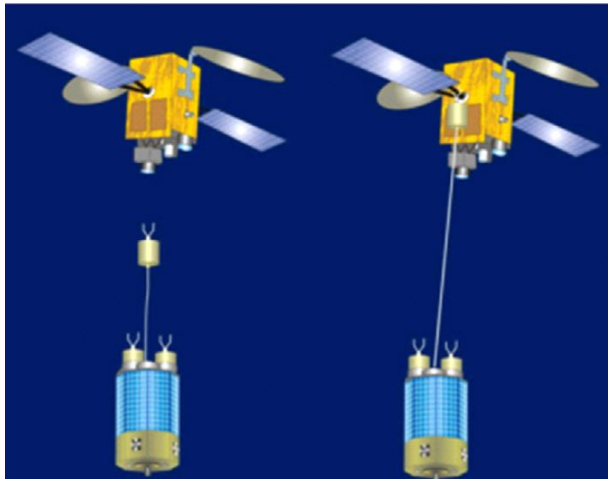

Tether capturing

Shan et al., Progress in Aerospace Science 2016

Contactless removal

Rubenchik et al., Light: Science and Applications, 2014

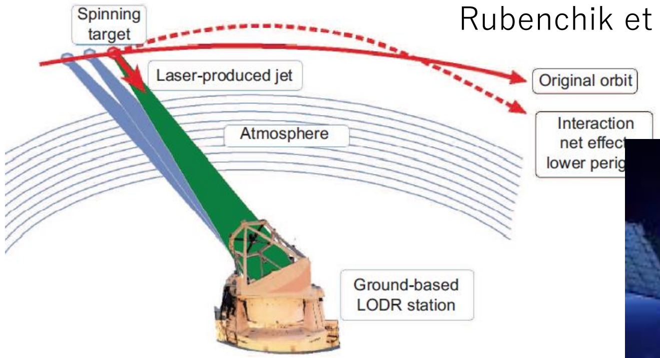

Laser-based removal

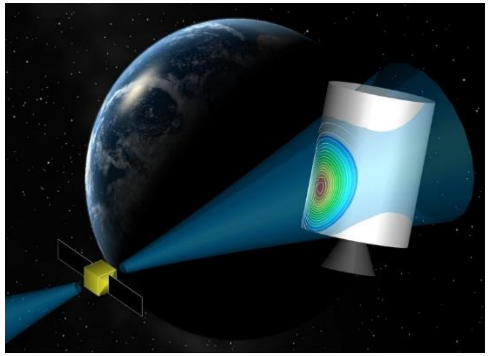

the ion beam shepherd (IBS)

Two propulsion devices are required (ion gridded thrusters)

Bombardelli and Pelaez, J. Guid. Control Dyn. 2011

Contactless debris removal using the bi-directional helicon thruster

SCIENTIFIC REPORTS

OPEN

Demonstrating a new technology for space debris removal using a bi-directional plasma thruster

d: 8 May 2018

Kazunori Takahashi[1], Christine Charles[2], Rod W. Boswell[2] & Akira Ando[1]

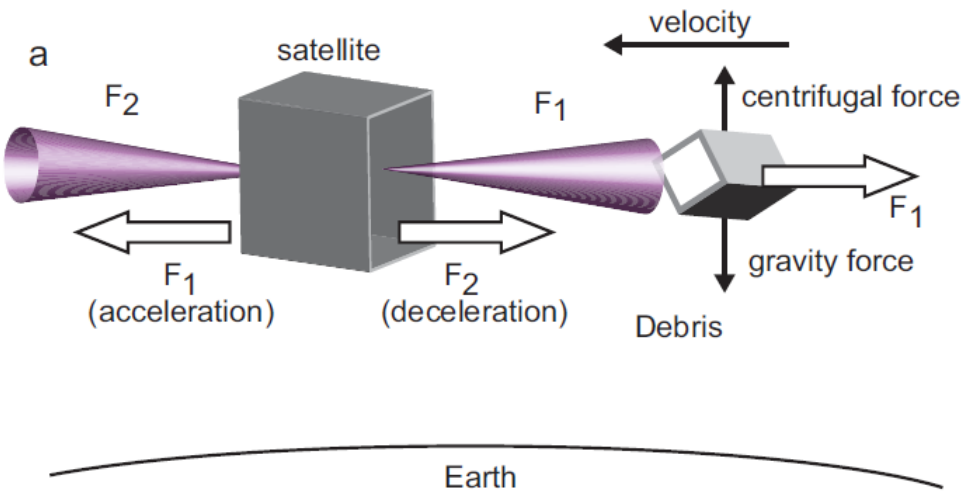

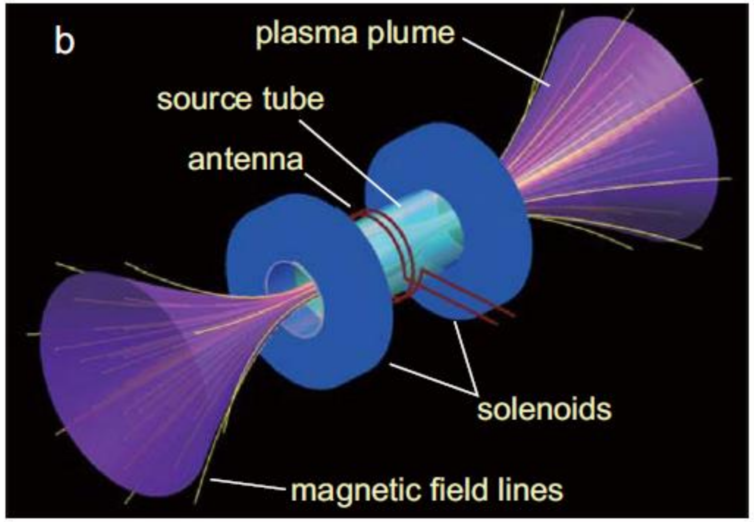

- All the modes of acceleration, deceleration, and debris removal modes are required for the actual space mission.
- High power electric propulsion is desired for the large size debris removal.

Laboratory setup and photos

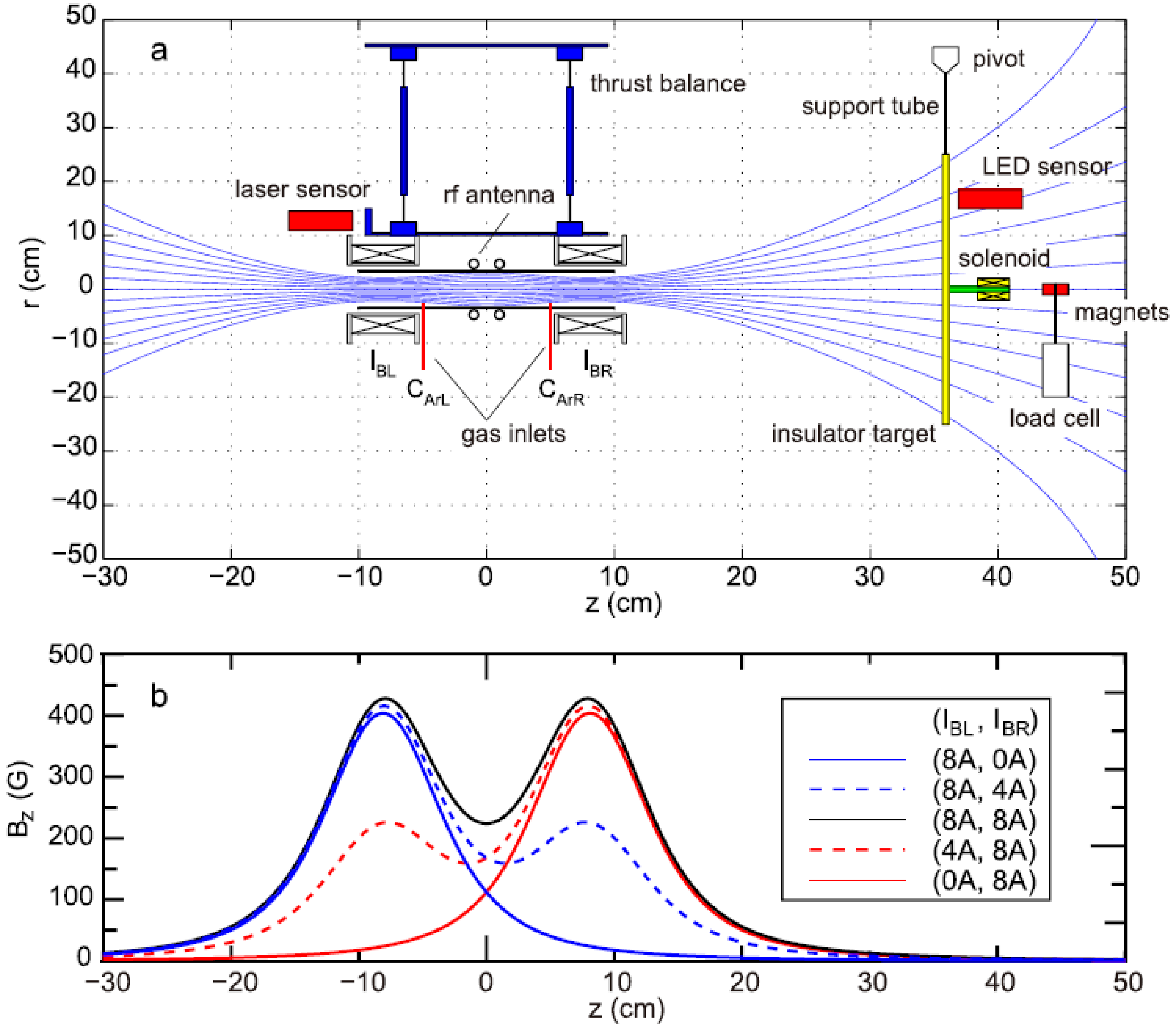

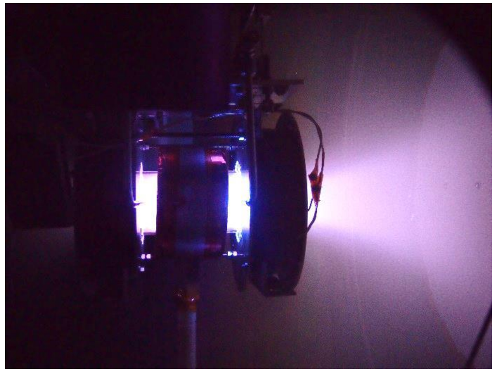

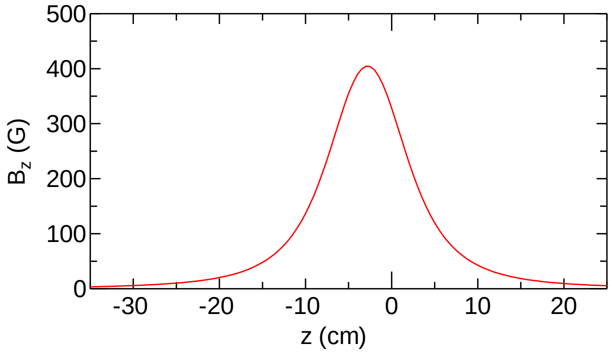

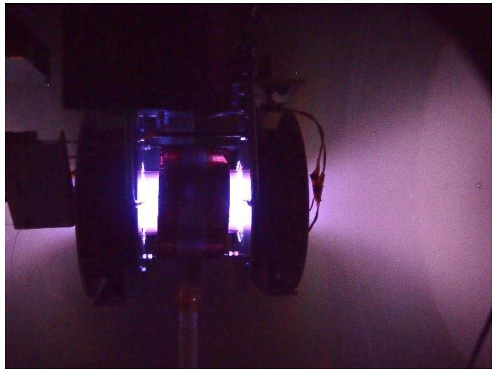

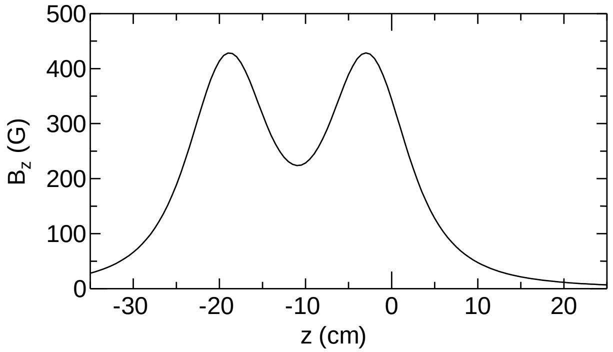

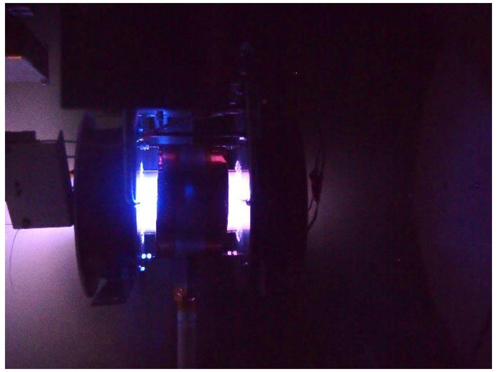

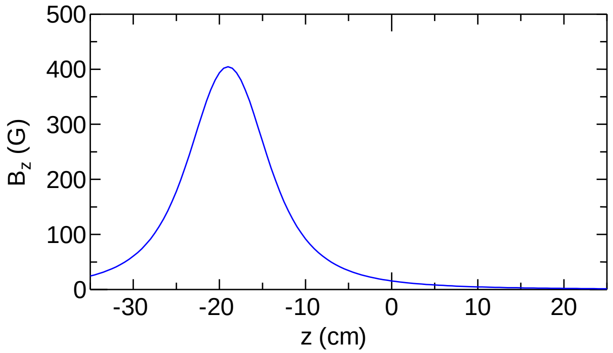

Switching the acceleration, deceleration, and debris removal modes

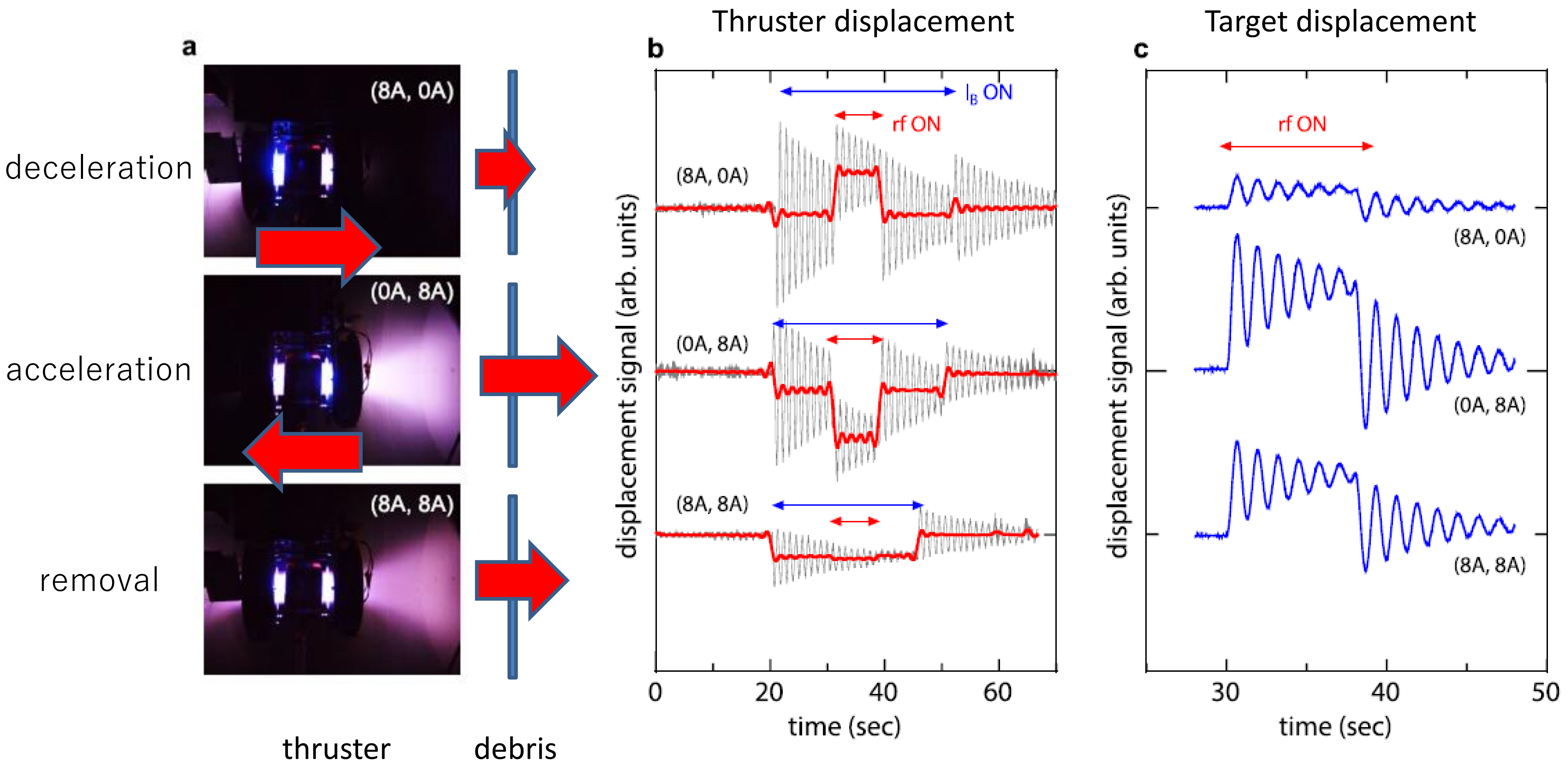

Takahashi, Charles, and Boswell, Scientific Reports, 2018

Continuous change in the thrust and force to the debris

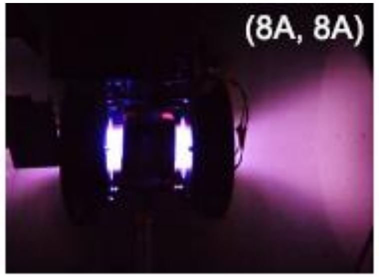

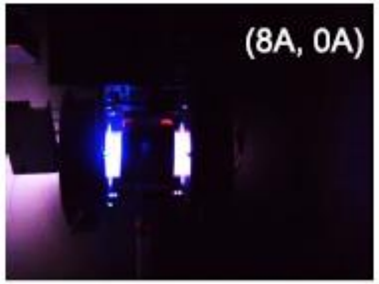

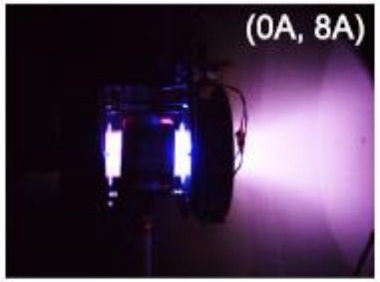

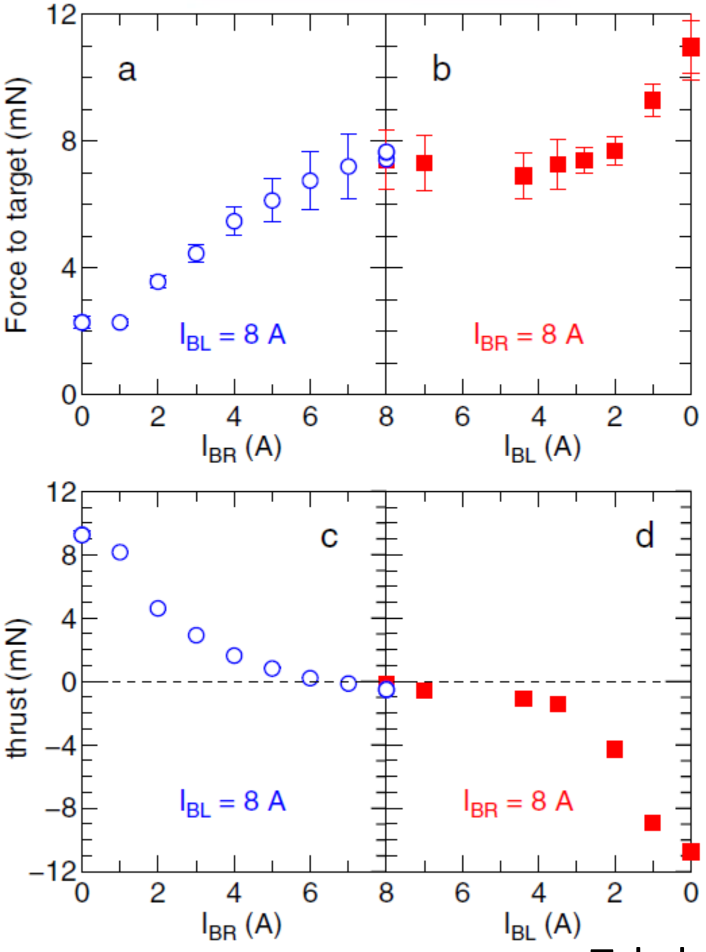

The thrust and the force to the debris can be continuously changed only by the solenoid currents.

Takahashi, Charles, and Boswell, Scientific Reports, 2018

Conclusion

- The studies on the magnetic nozzle rf plasma thruster (sometimes called a helicon thruster) has been progressed over the last decade, showing many aspects of physics.
- The thruster efficiency calculated from the rf power and the thrust is approaching ~ 30% in April 2022.
- There seem to be further interesting physics and engineering there, e.g., the plasma detachment from the MN, the thruster design, the system development (the rf system, the gas injection system, the magnet design, etc…). Although not shown here, the electron thermodynamics is also an important topic.
- There would be common technologies between the thruster and the industrial plasmas.
- Although not shown here, the automatically- and fast-controlled frequency tunable rf system is useful for both the thruster and the plasma etching reactor.

→ e.g. AIP Advances, 11, 025013 (2021) & Front. Phys., 9, 639010 (2021)